Characterization of a LanC-free pathway for the formation of an LL-MeLan residue and an *allo*AviMeCys residue in the newly identified class V lanthipeptide triantimycins

Weizhong Ding,[a,#] Xiaofeng Wang,[a,b,#] Yu Yin,[c] Jiang Tao,[d,*] Yanqing Xue[a,*] and Wen Liu[a,*]

[a]State Key Laboratory of Bioorganic and Natural Products Chemistry, Center for Excellence in Molecular Synthesis, Shanghai Institute of Organic Chemistry, University of Chinese Academy of Sciences, 345 Lingling Road, Shanghai 200032, China.
[b]School of Chemistry and Materials Science, Hangzhou Institute for Advanced Study, University of Chinese Academy of Sciences, 1 Sublane Xiangshan, Hangzhou 310024, China.
[c]School of Pharmacy, Shanghai Jiaotong University, Shanghai 200240, China.
[d]Department of General Dentistry, Shanghai Ninth People's Hospital, Shanghai Jiao Tong University School of Medicine, College of Stomatology, Shanghai Jiao Tong University; National Center for Stomatology, National Clinical Research Center for Oral Diseases, Shanghai Key Laboratory of Stomatology, Shanghai Research Institute of Stomatology, Research Unit of Oral and Maxillofacial Regenerative Medicine, Chinese Academy of Medical Science, No. 639 Zhizaoju Road, Shanghai 200011, China

[#] These authors contributed equally to this work.

Table of Contents.

3. Supplementary Tables.

4. References.

1. Supplementary Methods.

1.1 General Materials and Methods.

Materials, Bacteria Strains and Plasmids. Chemicals, biochemicals and media were purchased from Sinopharm Chemical Reagent Co., Ltd. (China), Oxoid Ltd. (U.K.) or Sigma-Aldrich Corporation (USA) unless otherwise stated. Enzymes and kits for DNA manipulations were purchased from Takara Bio (Japan), Vazyme Biotech (China) or Thermo Fisher Scientific (USA). Bacterial strains and plasmids are summarized in **Table S5**. Primers used in this study are listed in **Table S6**.

Chemical Analysis. ^{1}H NMR, and ^{13}C NMR spectra were recorded on an Agilent 500 MHz PremiumCompact^{+} NMR spectrometer (Agilent Technologies Inc., USA) or on a Bruker AV500 S5 spectrometer (Bruker Co. Ltd., Germany). Analyses by high-performance liquid chromatography (HPLC) was carried out on an Agilent 1260 HPLC system (Agilent Technologies Inc., USA). Semi-preparative HPLC was performed on Agilent 1100 system equipped with a DAD detector. Analysis by HPLC-coupled low resolution mass spectrometry (LR-MS) and high-resolution tandem MS (HR-MS/MS) were performed on a Thermo Fisher LTQ XL ESI-MS spectromer and a Q Exactive™ Plus Mass Spectrometer (Thermo Fisher Scientific Inc., USA). HR-ESI-MS analysis were carried out on an Agilent 6230B Accurate Mass TOF LC/MS System (Agilent Technologies Inc., USA). Related data were processed using Thermo Xcalibur software™ or Agilent MassHunter software™.

DNA Isolation, Manipulation, Sequencing and Synthesis. DNA isolation and manipulation in *Escherichia coli* or *Streptomyces* strains were carried out according to standard methods.[1] PCR amplifications were carried out on an Applied Biosystems Veriti™ Thermal Cycler either using Taq DNA polymerase (Vazyme Biotech, Nanjing, China) for routine genotype verification or KOD DNA polymerase (Takara Bio, Tokyo, Japan) for high fidelity amplification. Primer synthesis was performed at Shanghai

Biosune Biotech Co., Ltd. (Shanghai, China). DNA sequencing was performed at Shanghai Biosune Biotech Co., Ltd. (Shanghai, China).The *stn* cluster that contains *stnA1A2A3U1KYDXPJMU2* was chemically synthesized by GenScript (Nanjing, China).

1.2 Constructs for Heterologous Expression in *S. coelicolor.*

The *stn* cluster was separately synthesized and cloned into the empty plasmid pXY200-1 by GenScript (Nanjing, China), resulting the plasmid pXYDuet-*stn*. Precisely, the 7 genes including *orf2/stnK/stnY/stnA1/stnA2/stnA3/stnM* was synthesized under the first *tipA* promoter, which led to plasmid pXY200-1-*stn*-half. Then the left 5 genes including *stnJ/stnD/stnX/stnP/orf1* and the second *tipA* promoter were synthesized and cloned into the plasmid pXY200-1-*stn*-half, which resulted in the working construction pXYDuet-*stn* (see **Figure 2B**).

The DNA synthesis resulted plenty of "semi-cloned" plasmids which were easily used for gene deletion and/or base edition combining enzymatic digestion, new custom-DNA synthesis, and ligation. Thusly, the gene deletions and base editions within this work were conducted by GenScript (Nanjing, China). Plasmids used in this work were listed in **Table S5**.

The introduction of each above recombinant plasmid into *S. coelicolor* M1146 chassis was carried out by *E. coli* ET12567-*Streptomyces* conjugation,[1] yielding the corresponding recombinant strains listed in **Table S5**.

1.3 Compounds Production and Examination.

The growth and preservation of *S. coelicolor* M1146 and the recombinant strains were conducted according to the manual.[1] Briefly, MS medium was used for spore

production. The fresh spores of the *Streptomyces* strains were inoculated into 50 mL TSB medium containing 50 μg/mL of apramycin, and were grown at 30℃ and 220 rpm for 3 d，5 mL of the resulting seed culture was inoculated in 100 mL TSB medium with thiostrepton (to a final concentration of 5 μg/mL). After growth for 4 d at 30℃ and 220 rpm, 1 mL of the fermentation broth was centrifuged, and the collected mycelia were soaked in 1 mL of methanol for 30 min. After centrifugation, the methanol extract was subjected to HPLC-MS (positive ion mode) analysis on an Agilent SB-C18 Zorbax column (5 μm，4.6 mm × 250 mm) by gradient elution of solvent A (H_2O + 0.1% FA) and solvent B (CH_3CN + 0.1% FA) with a flow rate of 1 mL/min over a 36 min period: T = 0 min, 5 % B; T = 6 min, 5 % B; T = 25 min, 100 % B; T = 33 min, 100 % B; and T = 34 min, 5 % B; T = 36 min, 5 % B. Further HPLC coupled HR-MS/MS (positive ion mode) analysis was conducted on an Agilent Zorbax column (300SB-C18, 3.5 μm, 2.1 mm × 100 mm) by gradient elution of solvent A(H_2O + 0.1% FA) and solvent B (CH_3CN + 0.1% FA) at a flow rate of 0.3 mL/min over a 23 min period as follows: T = 0 min, 5 % B; T = 5 min, 5 % B; T = 15 min, 95 % B; T = 20 min, 95 % B; T = 23 min, 5 % B.

1.4 Compounds Purification and Characterization.

For compound **1** and **3** isolation, ~ 120 L of the TSB fermentation broth of the STN-10 strain was centrifuged, and pelleted mycelial cake was extracted with 5 L of methanol for three times. After concentration, the crude extract was subjected to a Sephadex LH - 20 column (Mitsubishi Chemical Corporation, Japan), and then eluted with methanol. After crude concentration, the semipreparation was conducted on an Agilent Pursuit XRs 5 - C18 column (250 mm × 21.2 mm) by isocratic elution (76 % methanol in H_2O with 0.1% TFA, 15.0 mL/min), and a WatersTM XBridge BEH C18 OBD Prep Column, (5 μm, 10 mm × 250 mm) by isocratic elution (59 % CH_3CN in H_2O with 0.1% FA, 3.0 mL/min), yielding ～10 mg of **1** and ～10 mg of **3** as white amorphous powder for NMR analysis. Key structural elements of compounds **1** and **3** were revealed based on

detailed 1D and 2D NMR spectra.

Similarly, compounds **3-1** and **1-T8S** were purified from 30 L of fermentation broth of the STN11 and STN12, respectively.

1.5 Chiral Analysis of Amino Acid Residues.

Chiral analysis of amino acid residues was conducted using the methods described previously. [2] For compound **1**, sample (400 μg in 600 μL of 6 M HCl, 5% thioglycolic acid (To prevent the degradation of Trp residue) [3] was heated to 110°C for 12 h with stirring in a sealed thick-walled reaction vessel, after which the hydrolysate was concentrated to dryness under N_2. The resulting hydrolysate was divided into two portions (200 μg × 2) for chemical derivatization with L-FDAA and D-FDAA, respectively. For compound **3**, sample (400 μg in 600 μL of 6 M HCl) was hydrolyzed as described above and the resulting hydrolysate was divided into two portions (200 μg × 2) for chemical derivatization with L-FDAA, respectively.

For L-FDAA and D-FDAA derivatization of amino acids, two aliquots (100 μg × 2) of the hydrolysate were treated with 1 M $NaHCO_3$ (100 μL) and L-FDAA or D-FDAA (1% solution in acetone, 100 μL) at 40°C for 1 h, respectively. Samples were neutralized with 1 M HCl (100 μL), diluted with MeCN (100 μL), and centrifuged (17000g for 10 min) prior to HPLC-MS analysis on an Aglient Eclipse Plus C18 column (250 × 4.6 mm, 5 μm) with gradient elution (at a flow rate of 1.0 mL/min from 10 % MeCN/H_2O to 60 % MeCN with 0.1 % FA over a 50 min period, 340 nm detector, positive ion mode). The configuration of the amino acid residues was determined by comparison of their retention times and elution orders with those for FDAA derivatives of amino acid standards. To prepare L-FDAA-amino acid standard derivatives, 50 mM of D- and L-amino acid (D/L-Ala, D/L-Val, D/L-Leu, D/L-Phe, D/L-Pro, D/L-Trp, D/L-Tyr, D/L-Met, D/L-Lys, D/L-Asp, D/L-Lys, D/L-Abu) dissolved in H_2O (50 μL) was treated with 1 M

$NaHCO_3$ (20 μL) and 1 % L-FDAA (100 μL) at 37°C for 2 h, and to prepare D-FDAA-Ala derivatives, 50 mM of D/L-Ala, dissolved in H_2O (50 μL) was treated with 1 M $NaHCO_3$ (20 μL) and 1 % D-FDAA (100 μL) at 37°C for 2 h, respectively. After reaction, the solution was quenched with 1 M HCl (20 μL) and diluted with MeCN (810 μL) for HPLC-MS analysis using the same column and elution conditions as above.

The L-FDAA derivatization of LL- and DL-Lan and LL- and DL-MeLan amino acids were synthesized according to ref 5. The synthetic procedure was described in **1.7**.

1.6 Iodoacetamide Derivatization.

The number of free cysteines in the modified mStnA1-1 and mStnA3 peptides was determined through the alkylation of unreacted Cys thiols with IAA. The reaction was performed in reaction buffer (50 mM Tris pH = 8.0, 1mM TCEP, 10 mM IAA with peptide concentrations ranging from 50-100 μM) at room temperature for 2 h. The reaction mixture was centrifuged and then were analyzed by HPLC-MS.

1.7 Chemical Synthesis of DL/LL-(Me)Lan Standard Derivatives.

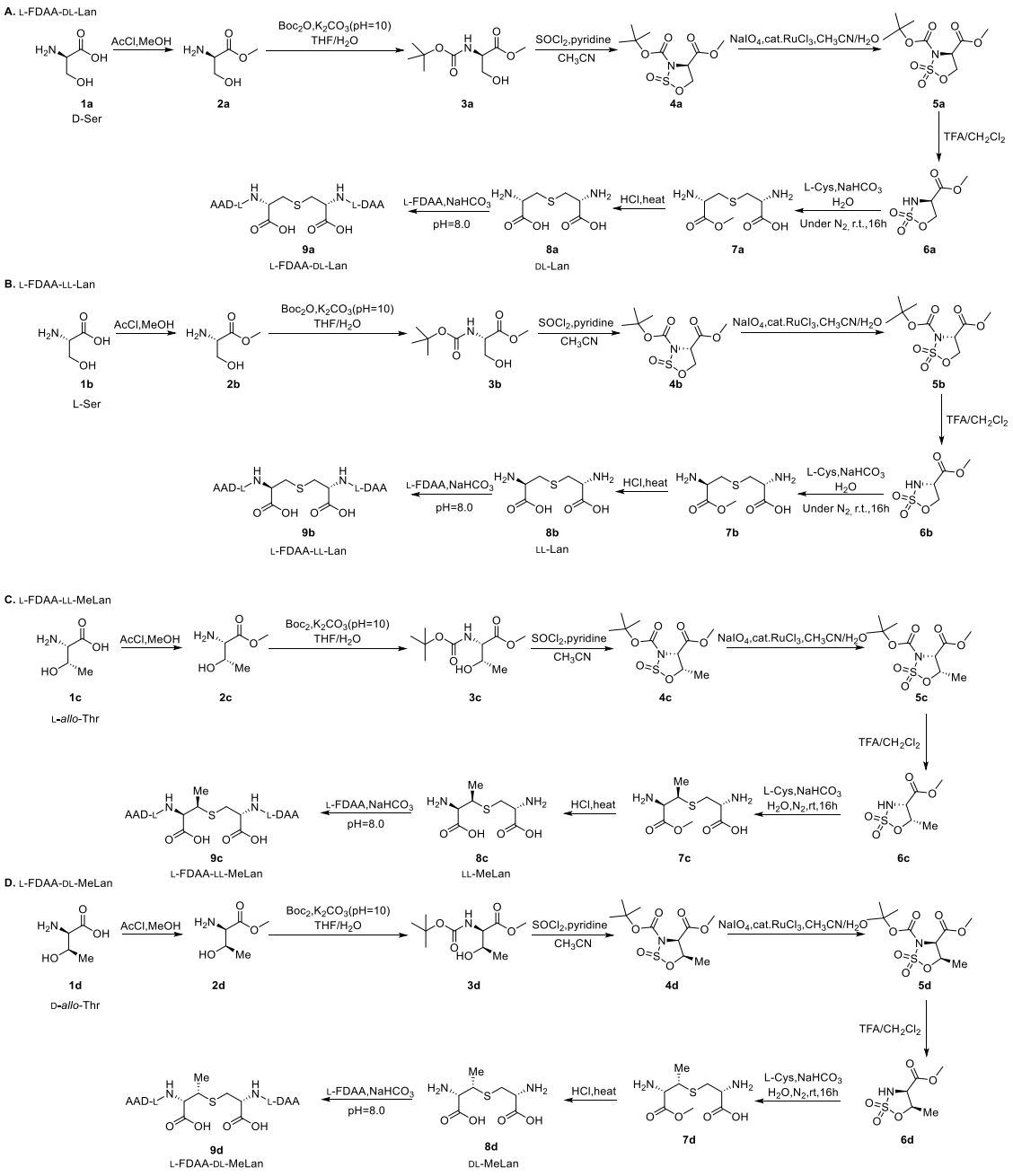

Synthesis of (2*S*, 6*R*)-Lan (DL-Lan, **A**) and (2*R*, 6*R*)-Lan (LL-Lan, **B**) standard derivatives was performed according to a previous report, [5] and (2*R*, 3*R*, 6*R*)-Lan (LL-MeLan, **C**) and (2*S*, *3S*, 6*R*)-Lan (DL-MeLan, **D**) was synthesized accordingly with

minor adaption.

For DL-Lan derivatives (**A**), D-serine (**1a**) serve as the starting material. Acetyl chloride (AcCl, 4 ml, 60 mmol) was slowly added to MeOH (25 ml) at 0 ℃. The solution was stirred for 30 min, followed by addition of D-serine (2.1 g, 20 mmol). After refluxing for 3 h, the solution was cooled to room temperature, and evaporated under reduced pressure to **2a** as a white solid.

2a was resolved in water (12 mL, followed by addition of K_2CO_3 (2.76 g, 20 mmol, pH = 10). After addition of the solution of Boc_2O (5.23 g, 24 mmol) in tetrahydrofuran (THF, 28 mL), the mixture was stirred for 16 h. THF was evaporated away, and the left aqueous solution was extracted with EtOAc (3 x 40 ml). The organic fraction was washed with water and brine, respectively, and then dried over $MgSO_4$, filtered, and evaporated under reduced pressure to yield **3a** as a colorless transparent oil.

$SOCl_2$ (2.8 mL, 37.5 mmol) was added to degassed CH_3CN (20 mL) in a dry round bottom flask under nitrogen. The solution was cooled to -42 ℃. **3a** (15 mmol) in degassed CH_3CN (20 mL) was added dropwise in 30 min. After the addition of pyridine (6 ml, 75 mmol) in 10 min, the yellow mixture was stirred for 2 h at -42 ℃ and then the mixture was stirred for 8 h at room temperature (r. t.). Ice was added to quench the reaction. The solution was acidified with aqueous 10% $NaHSO_4$ (pH = 1). The aqueous layer was extracted with EtOAc (3 x 40 mL). The organic fraction was washed with

water, saturated $NaHCO_3$ and brine, respectively, and then dried over $MgSO_4$, filtered, and evaporated under reduced pressure to yield **4a** as a yellow oil.

4a was dissolved in 20 mL CH_3CN. $RuCl_3$. xH_2O (30 mg), $NaIO_4$ (3.52g. 17.5 mmol), H_2O (20 mL) were added to the solution at 0 ℃. The solution was stirred for 30 min at 0 ℃ and returned to room temperature for 8 h. After the addition of EtOAc (20 mL) and brine (20 mL), the solution was extracted with EtOAc (3 x 40 mL). The organic fraction was washed with water, saturated $NaHCO_3$ and brine, respectively. The organic layer was dried over $MgSO_4$, filtered, and evaporated under reduced pressure to yield **5a** as a colorless transparent oil.

5 mL TFA was added to the solution of **5a** in 5 mL CH_2Cl_2. After refluxing for 30 min, the volatiles were removed in vacuo to obtain **6a**, which was added to the degassed solution of $KHCO_3$ (5 g, 50 mmol), followed by the addition of L-cysteine (1.2 g, 10 mmol, 25 ml H_2O). The solution was stirred for 16 h at room temperature prior to the addition of concentrated HCl (37% HCl, 25 mL, 250 mmol). Then, the acidic solution was heated under N_2 at 70 ℃ for 5 h. The solution was then adjusted to pH= 6.0 by NaOH, and the resulting DL-Lan (**8a**) was collected as white precipitate by filtration.

8a (0.21 mg, 1 mM) treated with 1 M $NaHCO_3$ (20 μL) and 1 % L-FDAA (100 μL) at 37°C (pH = 8.0) for 2h to yield L-FDAA-DL-Lan (**9a**).

The synthesis of L-FDAA-LL-Lan (**9b**), L-FDAA-LL-MeLan (**9c**), and L-FDAA-DL-MeLan (**9d**) was conducted accordingly, except for using L-serine (**1b**), L-*allo*-threonine (**1c**), and D-*allo*-threonine (**1d**) as the starting materials, respectively.

Spectra of key intermediates:

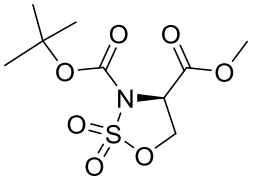

5a: ^{1}H NMR (500 MHz, $CDCl_3$) 4.85 – 4.65 (m, 3H), 3.85 (s, 3H), 1.55 (s, 9H). ^{13}C NMR (126 MHz, $CDCl_3$) δ 167.57 (s), 148.25 (s), 86.30 (s), 67.50 (s), 57.10 (s), 53.85 (s), 27.32 (s). HRMS m/z (ESI+). $[M+NH_4]^+$ calc 299.0907; found 299.0906.

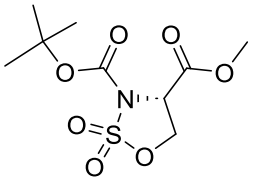

5b: ^{1}H NMR (500 MHz, $CDCl_3$) 4.88 – 4.67 (m, 3H), 3.84 (s, 3H), 1.57 (s, 9H). ^{13}C NMR (126 MHz, $CDCl_3$) δ 166.87 (s), 148.55 (s), 86.60 (s), 67.30 (s), 57.05 (s), 53.65 (s), 27.12 (s). HRMS m/z (ESI+). $[M+NH_4]^+$ calc 299.0907; found 299.0905.

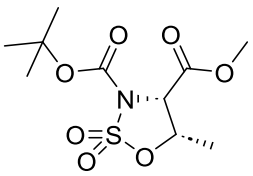

5c: ^{1}H NMR (500 MHz, $CDCl_3$) δ 5.09 (p, J = 6.3 Hz, 1H), 4.70 – 4.53 (d, 1H), 3.82 (s, 3H), 1.49 (s, 9H), 1.46 (d, J = 5.0 Hz, 3H). ^{13}C NMR (126 MHz, $CDCl_3$) δ 166.57 (s), 148.23 (s), 86.20 (s), 62.30 (s), 53.10 (s), 27.85 (s), 15.32 (s). HRMS m/z (ESI+). $[M+NH_4]^+$ calc 313.1064; found 313.1074.

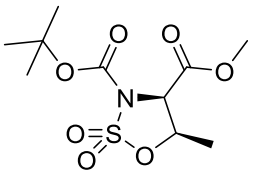

5d: ^{1}H NMR (600 MHz, $CDCl_3$) δ 5.15 (p, J = 6.3 Hz, 1H), 4.71 (d, J = 6.0 Hz, 1H), 3.86 (s, 3H), 1.52 (s, d, J = 5.1 Hz, 12H). ^{13}C NMR (126 MHz, $CDCl_3$) δ 166.68 (s), 148.23 (s), 86.11 (s), 65.01 (s), 53.08 (s), 27.84 (s), 21.04 (s). HRMS m/z (ESI+). $[M+NH_4]^+$ calc 313.1064; found 313.1074.

1.8 Genes Co-Expression in *E. coli* and Protein Purification.

Constructs for co-expression in *E. coli*. Related *stn* genes were amplified using corresponding primers pairs listed in **Table S6**. While the PCR product containing *stnA1* or *stnA3* was cloned into the plasmid pRSFduet-1, the products containing *stnD* and/or *stnX* were cloned individually into pETduet-1 (see **Table S5**).

Protein expression. *E. coli* BL21(DE3) served as a general host for heterologous expression. The culture of each recombinant *E. coli* strain was incubated in LB medium (5 g of yeast extract, 10 g of tryptone and 10 g of NaCl per liter) containing 50 μg/mL kanamycin, 100 μ g/mL ampicillin, at 37 °C and 220 rpm until the cell density reached 0.6-0.8 at OD600. Protein expression was induced by the addition of isopropyl-*β*-D-thiogalactopyranoside (IPTG) to a final concentration of 0.1-0.3 mM, followed by further incubation for 25-30 hr at 25 °C or 16 °C. The cells were harvested by centrifugation at 5000 × g for 20 min, flash frozen and then stored at -80 °C.

Purification of a modified precursor peptide with SUMO tag. *E. coli* cells were re-suspended in lysis buffer (50 mM Tris-HCl, 100 mM NaCl and 5 mM imidazole, pH 7.5). Recombinant proteins that contain a 6 x His-tag were purified on a His Trap HP column (GE Healthcare, USA), which was pre-treated with 10 column volumes (CVs) of lysis buffer followed by 10 CVs of wash buffer (50 mM Tris-HCl, 100 mM NaCl and 20 mM imidazole, pH 7.5), using elution buffer (50 mM Tris-HCl, 100 mM NaCl and 250 mM imidazole, pH 7.5). Desired protein fractions were concentrated (to 500 μM-1 mM) using Amicon® Ultra-15 Centrifugal Filter Devices (MILLIPORE, USA) and desalted using a PD-10 Desalting Column (GE Healthcare, USA) according to the manufacturer's protocols, and then quantified in concentration by Bradford assay using bovine serum albumin as the standard. The purity of recombinant proteins was determined by sodium dodecyl sulfate polyacrylamide gel electrophoresis (SDS-PAGE).

1.9 Bioinformatic Analysis.

The bioinformatic survey of class Va lanthipeptides were conducted using cblaster tool.[6] Protein function analysis was carried out using available BLAST methods (http://www.ncbi.nlm.nih.gov/blast/). The sequence similarity analysis (SSN) was conducted using the EFI tools.[7] The multiple sequence alignment was performed by Clustal Omega tools (https://www.ebi.ac.uk/jdispatcher/msa/clustalo). The conserved core sequence analysis was generated by WebLogo 3.[8]

2. Supplementary Figures.

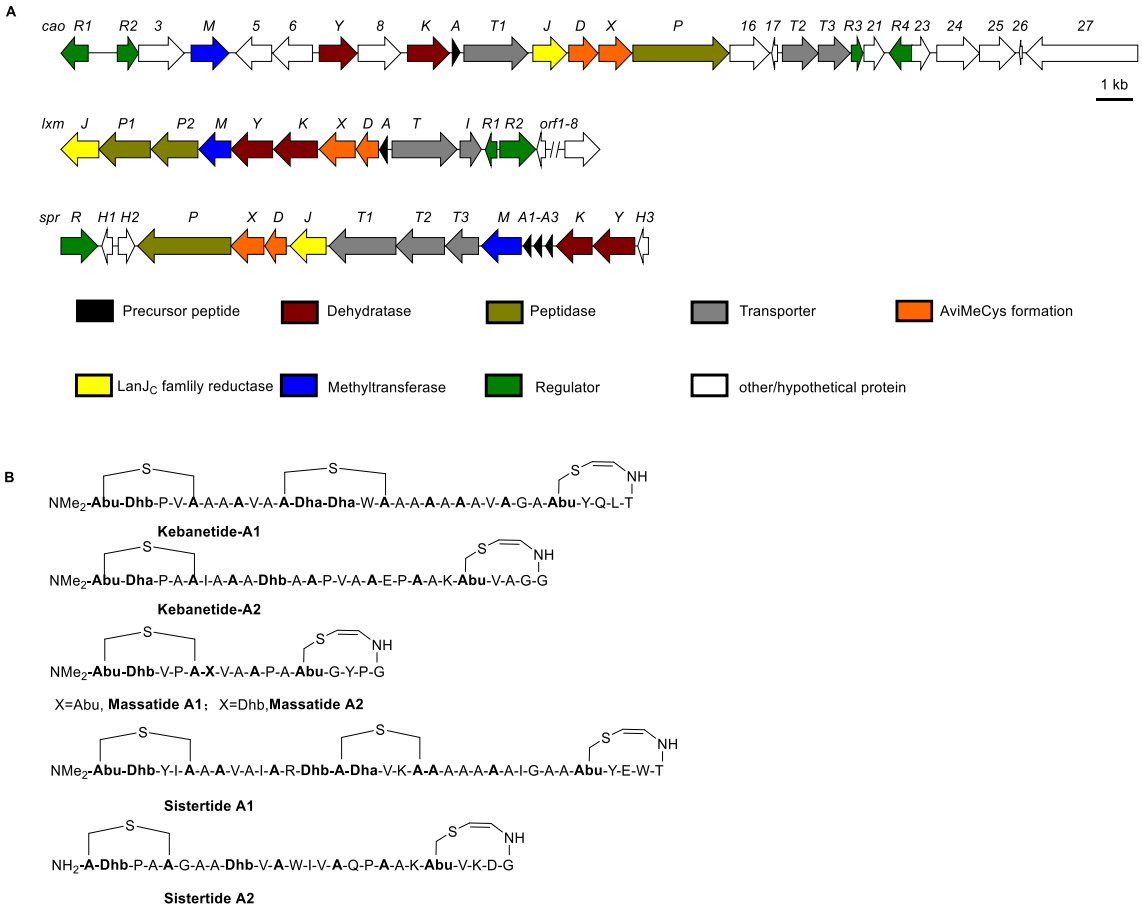

Figure. S1. Biosynthetic gene clusters of known class Va lanthipeptides (A), and recently reported class Va lanthipeptide members (B).

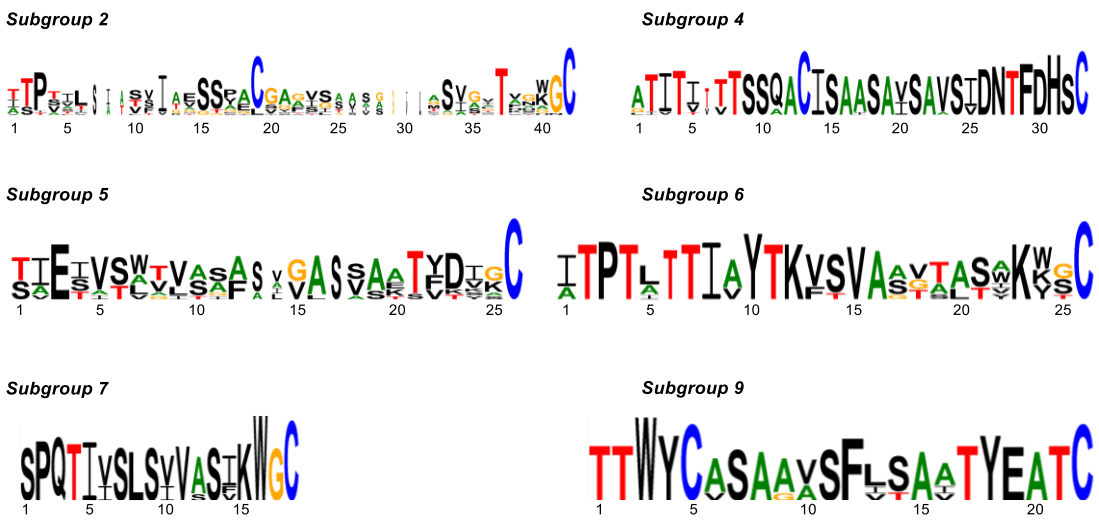

Figure S2. Conserved core sequence analysis of class Va candidates. The sequences of the precursor candidates are listed in **Table S1**.

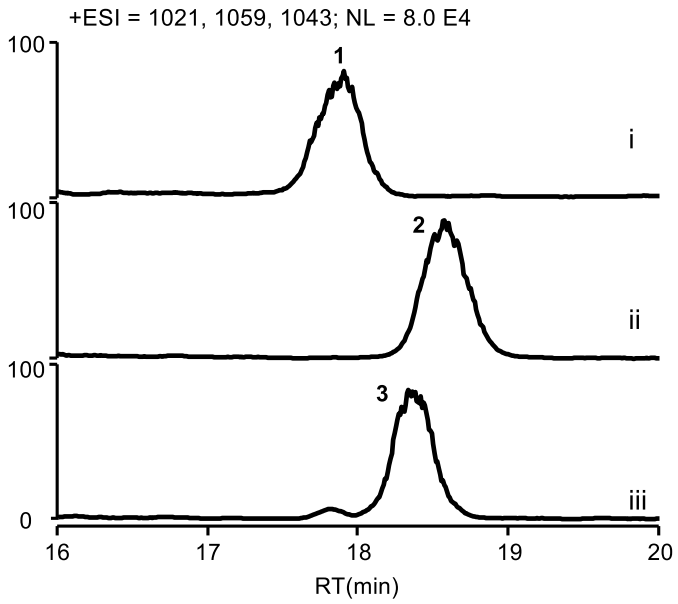

Figure. S3. HPLC-MS traces of the Δ*stnA1A2*, Δ*stnA1A3*, and Δ*stnA2A3* strains. (i), Δ*stnA2A3* strain. (ii), Δ*stnA1A3* strain. (iii), Δ*stnA1A2* strain. For compounds **1**, **2** and **3**, the m/z values are 1021, 1059, and 1043, respectively.

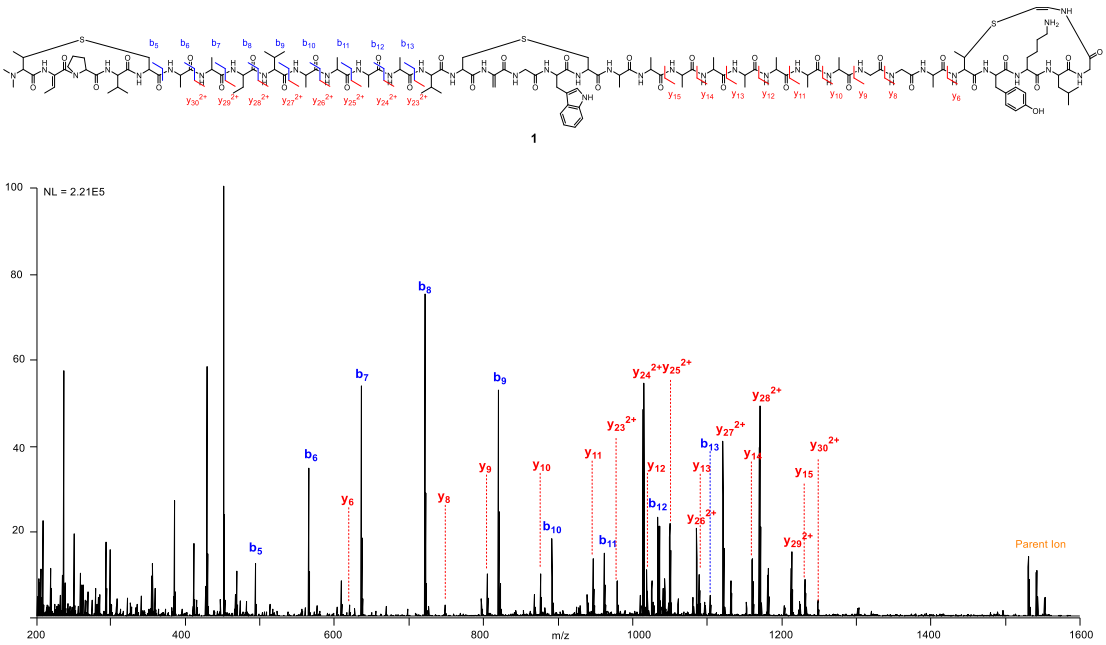

Ions	Calc.	Obs.	Er.(ppm)	Ions	Calc.	Obs.	Er.(ppm)
b5	494.2415	494.2426	2.2	**y30^{2+}**	1248.6171	1248.6123	3.8
b6	565.2786	565.2796	1.8	**y29^{2+}**	1213.0985	1213.0971	1.2
b7	636.3157	636.3166	1.4	**y28^{2+}**	1170.5721	1170.5707	1.2
b8	721.3685	721.3690	0.7	**y27^{2+}**	1121.038	1121.0372	0.7
b9	820.4369	820.4373	0.5	**y26^{2+}**	1085.5194	1085.5181	1.2
b10	891.474	891.4751	1.2	**y25^{2+}**	1050.0009	1049.9997	1.1
b11	962.5111	962.5115	0.4	**y24^{2+}**	1014.4823	1014.4816	0.7
b12	1033.5482	1033.5481	0.1	**y23^{2+}**	978.9637	978.9627	1.0
b13	1104.5853	1104.5883	2.7	**y15**	1231.6246	1231.6233	1.1
				y14	1160.5875	1160.5868	0.6
				y13	1089.5504	1089.5498	0.6
				y12	1018.5133	1018.5113	2.0
				y11	947.4762	947.4750	1.3
				y10	876.4391	876.4382	1.0
				y9	805.402	805.4010	1.2
				y8	748.3805	748.3801	0.5
				y6	620.3219	620.3220	0.2

Figure. S4. Tandem MS analysis of **1**. The HCD fragments and the MS/MS spectrum are shown.

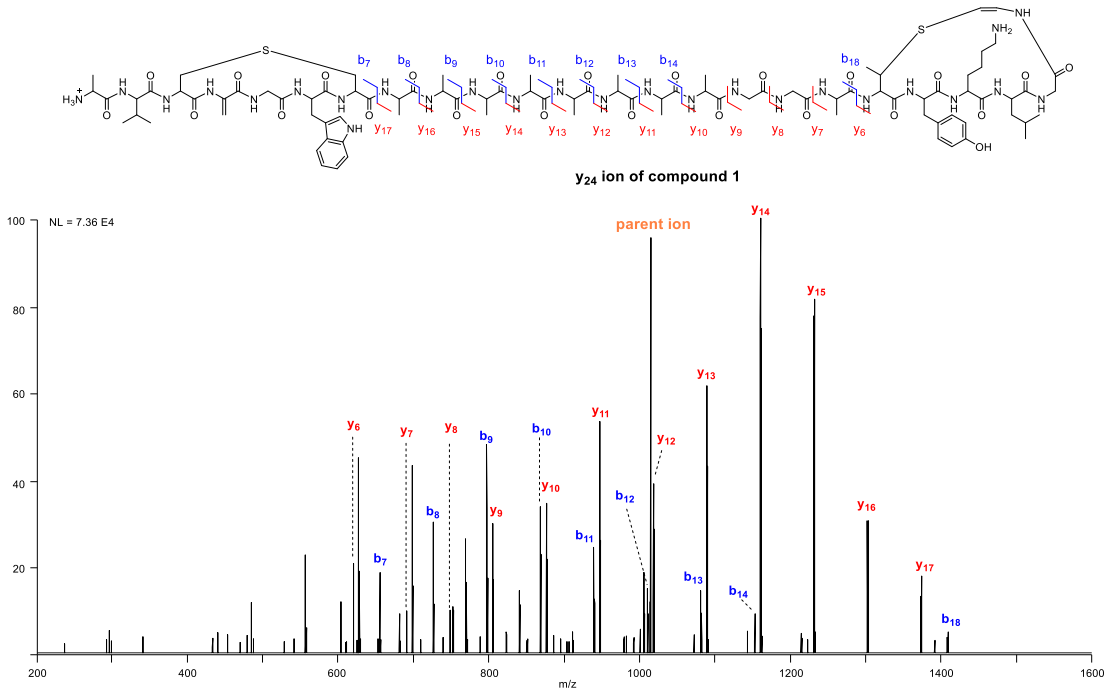

Ions	Calc.	Obs.	Er.(ppm)	Ions	Calc.	Obs.	Er.(ppm)
b7	655.2662	655.2682	3.1	**y17**	1373.6989	1373.6898	6.6
b8	726.3033	726.3011	3.0	**y16**	1302.6617	1302.6631	1.1
b9	797.3405	797.3393	1.5	**y15**	1231.6246	1231.6265	1.5
b10	868.3776	868.3791	1.7	**y14**	1160.5875	1160.5867	0.7
b11	939.4147	939.4124	2.4	**y13**	1089.5504	1089.5511	0.6
b12	1010.4518	1010.4426	9.1	**y12**	1018.5133	1018.5146	1.3
b13	1081.4889	1081.4864	2.3	**y11**	947.4762	947.4739	2.4
b14	1152.5260	1152.5238	1.9	**y10**	876.4391	876.4382	1.0
b18	1408.6432	1408.6445	0.9	**y9**	805.4020	805.4031	1.4
				y8	748.3805	748.3769	4.8
				y7	691.3590	691.3573	2.5
				y6	620.3219	620.3179	6.4

Figure. S5. Pseudo-MS^3 analysis of y24 of **1**. The HCD fragments and the MS/MS spectrum are shown.

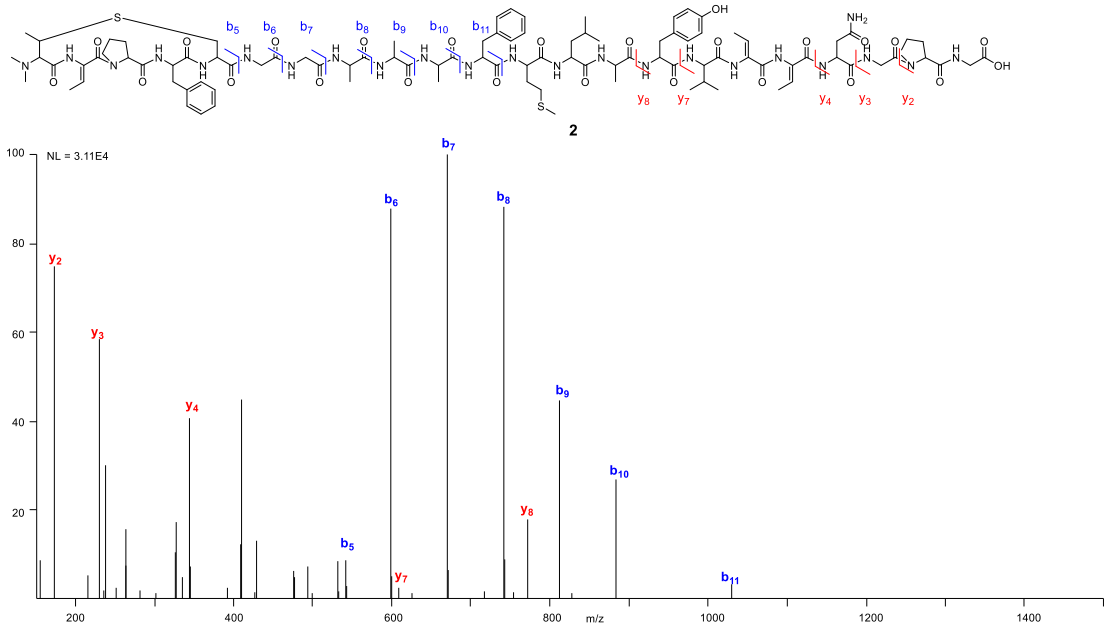

Ions	Calc.	Obs.	Er.(ppm)	Ions	Calc.	Obs.	Er.(ppm)
b5	542.2415	542.2438	4.2	**y8**	772.3619	772.3627	1.0
b6	599.2630	599.2656	4.3	**y7**	609.2985	609.2986	0.2
b7	670.3001	670.3027	3.9	**y4**	344.1559	344.1569	2.9
b8	741.3372	741.3397	3.4	**y3**	230.1130	230.1139	3.9
b9	812.3743	812.3770	3.3	**y2**	173.0915	173.0923	4.6
b10	883.4114	883.4137	2.6				
b11	1030.4799	1030.4813	1.4				

Figure. S6. Tandem MS analysis of **2**. The HCD fragments and the MS/MS spectrum are shown.

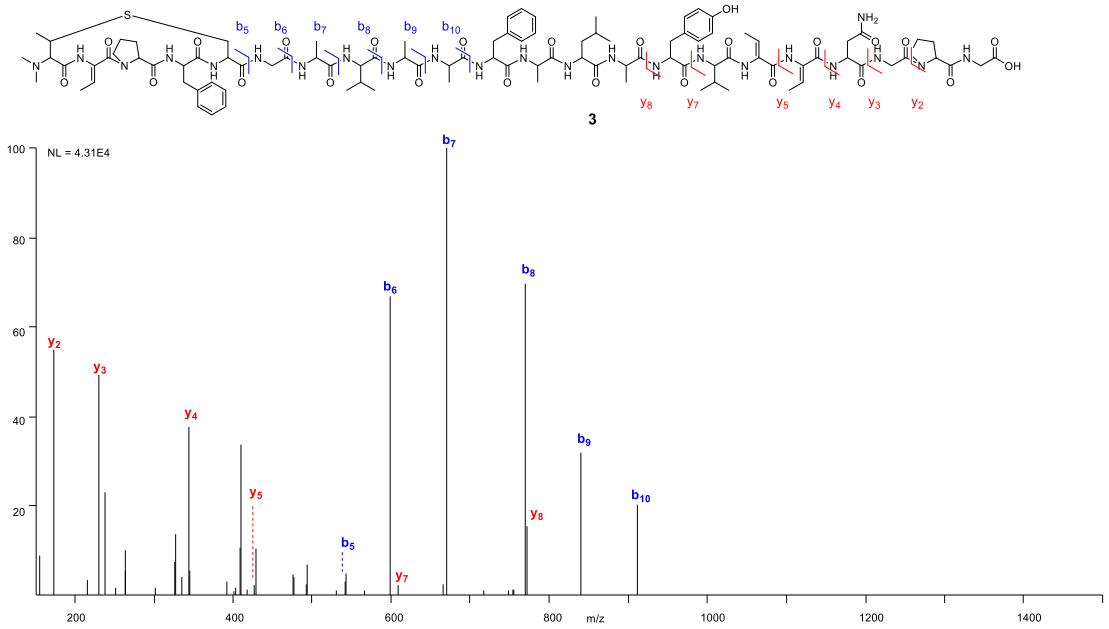

Ions	Calc.	Obs.	Er.(ppm)	Ions	Calc.	Obs.	Er.(ppm)
b5	542.2415	542.2427	2.2	**y8**	772.3619	772.3626	0.9
b6	599.2630	599.2656	4.3	**y7**	609.2985	609.2998	2.1
b7	670.3001	670.3029	4.2	**y5**	427.193	427.1942	2.8
b8	769.3685	769.3711	3.4	**y4**	344.1559	344.1569	2.9
b9	840.4056	840.4081	3.0	**y3**	230.113	230.1139	3.9
b10	911.4427	911.4452	2.7	**y2**	173.0915	173.0923	4.6

Figure. S7. Tandem MS analysis of **3**. The HCD fragments and the MS/MS spectrum are shown.

(A), Key 2D correlations of **1**.

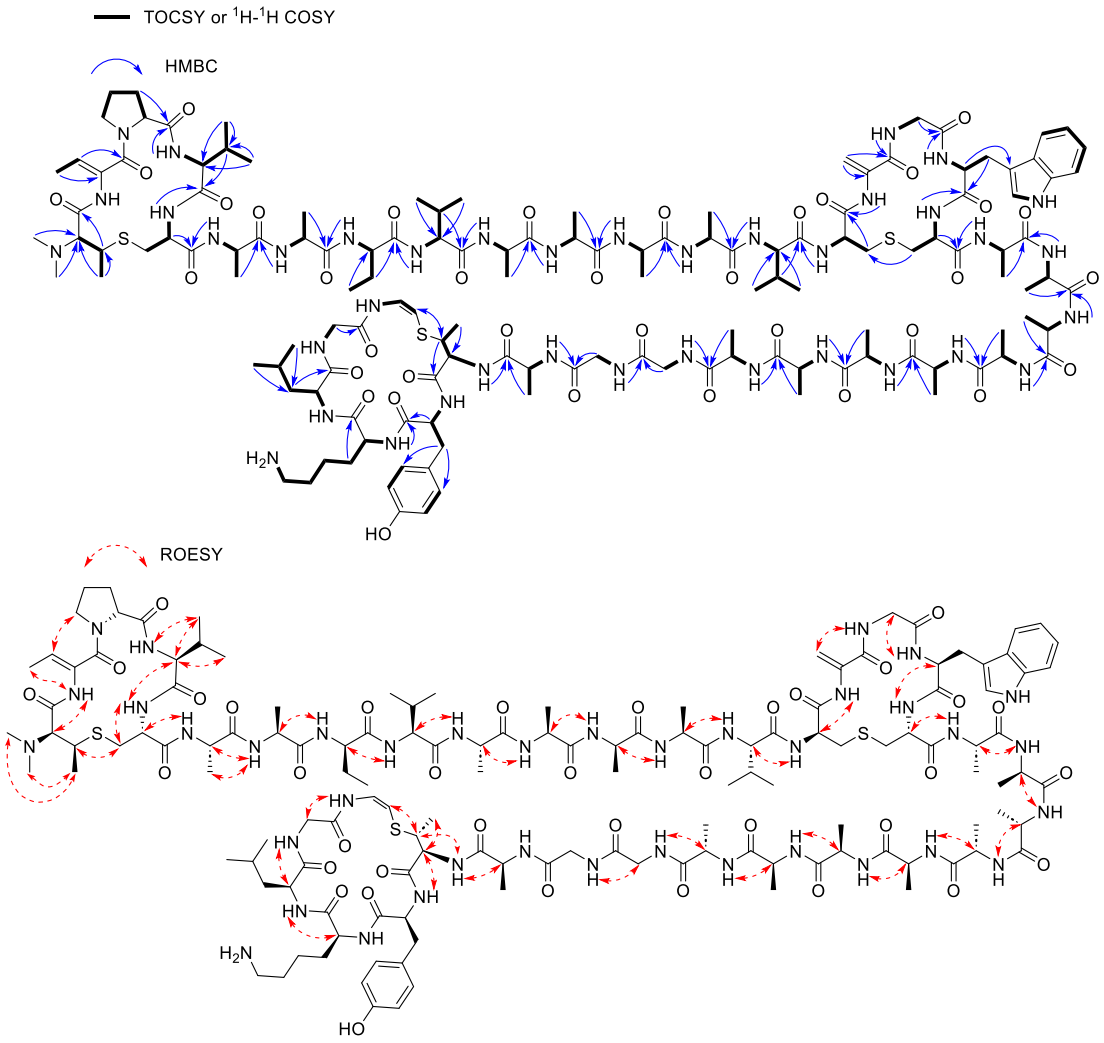

(B), 1D and 2D NMR spectra of **1** in DMSO-d_6.

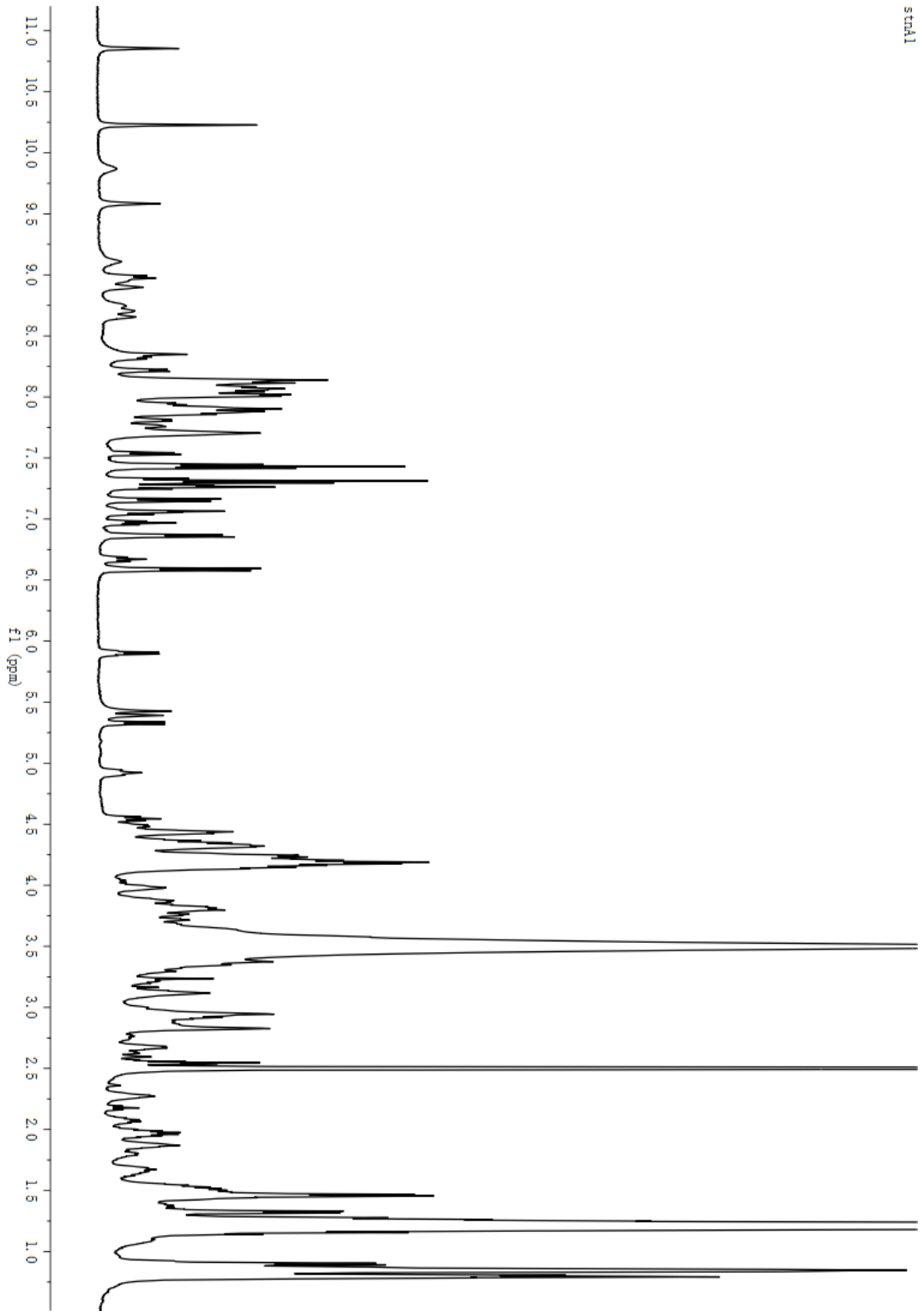

(i), ^{1}H NMR spectrum (full spectrum) of **1** in DMSO-d_6.

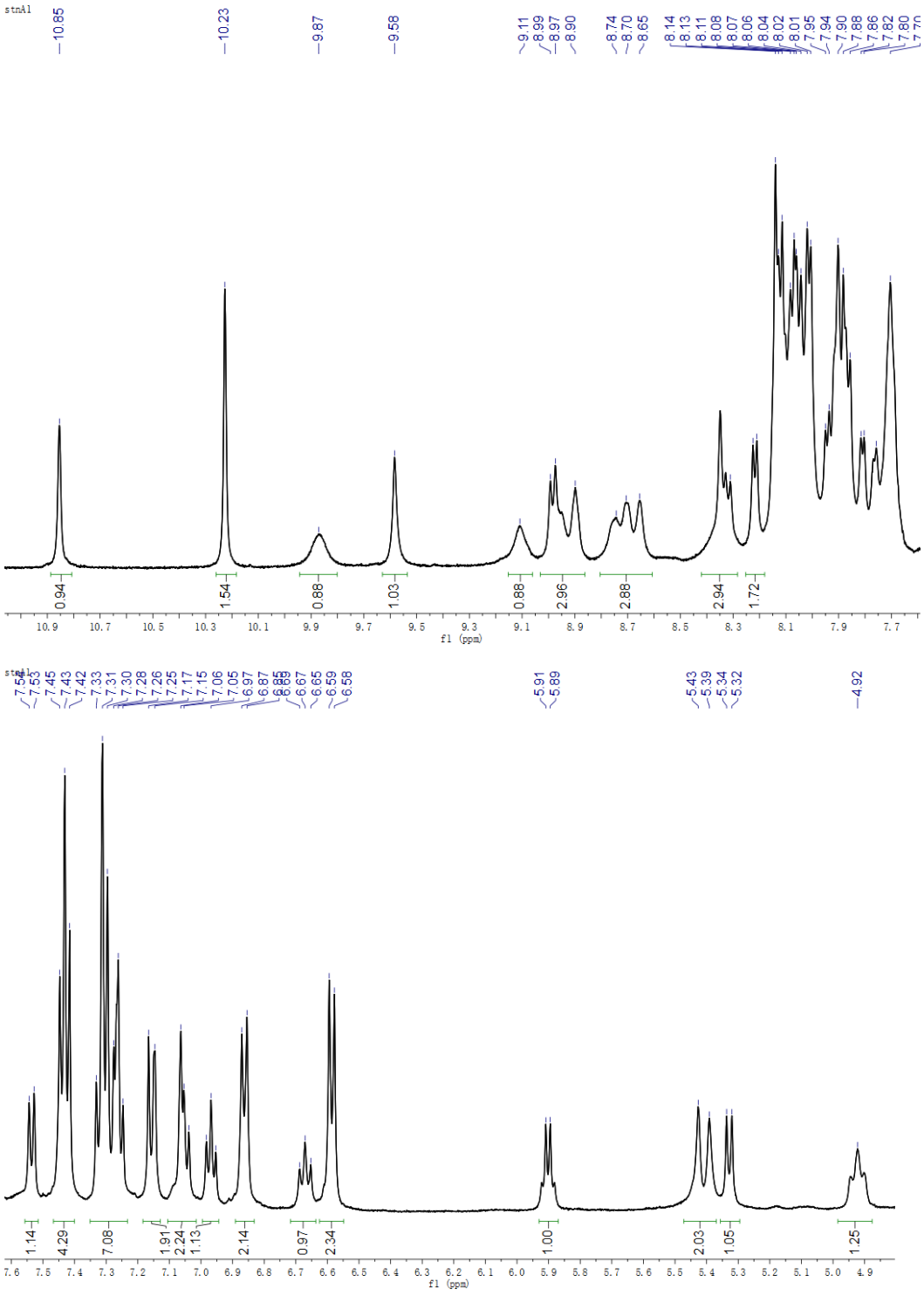

(ii), Localized zoom-in of ^{1}H NMR spectrum of **1** in DMSO-d_6.

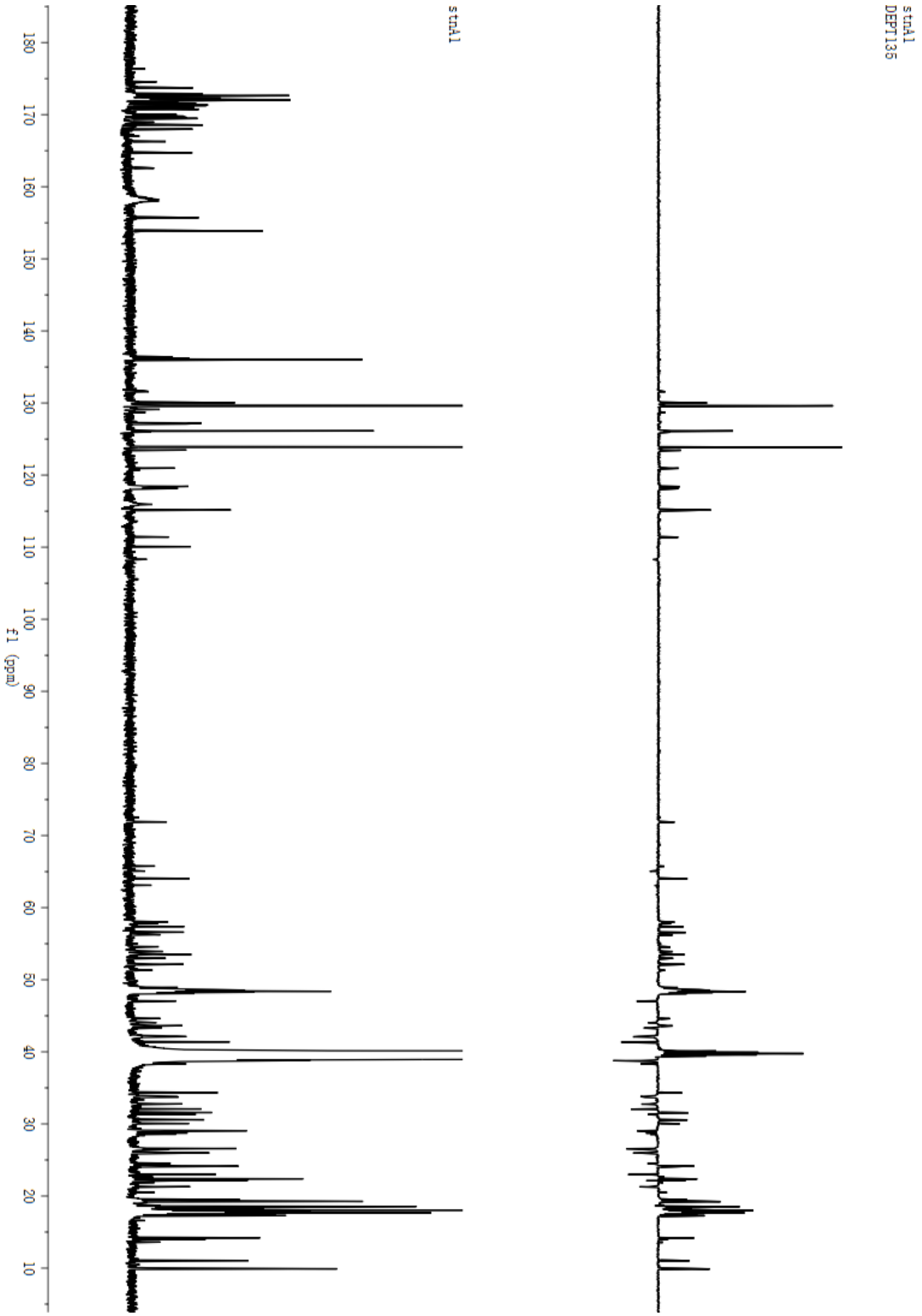

(iii), ^{13}C NMR spectrum (full spectrum) of **1** in DMSO-d_6.

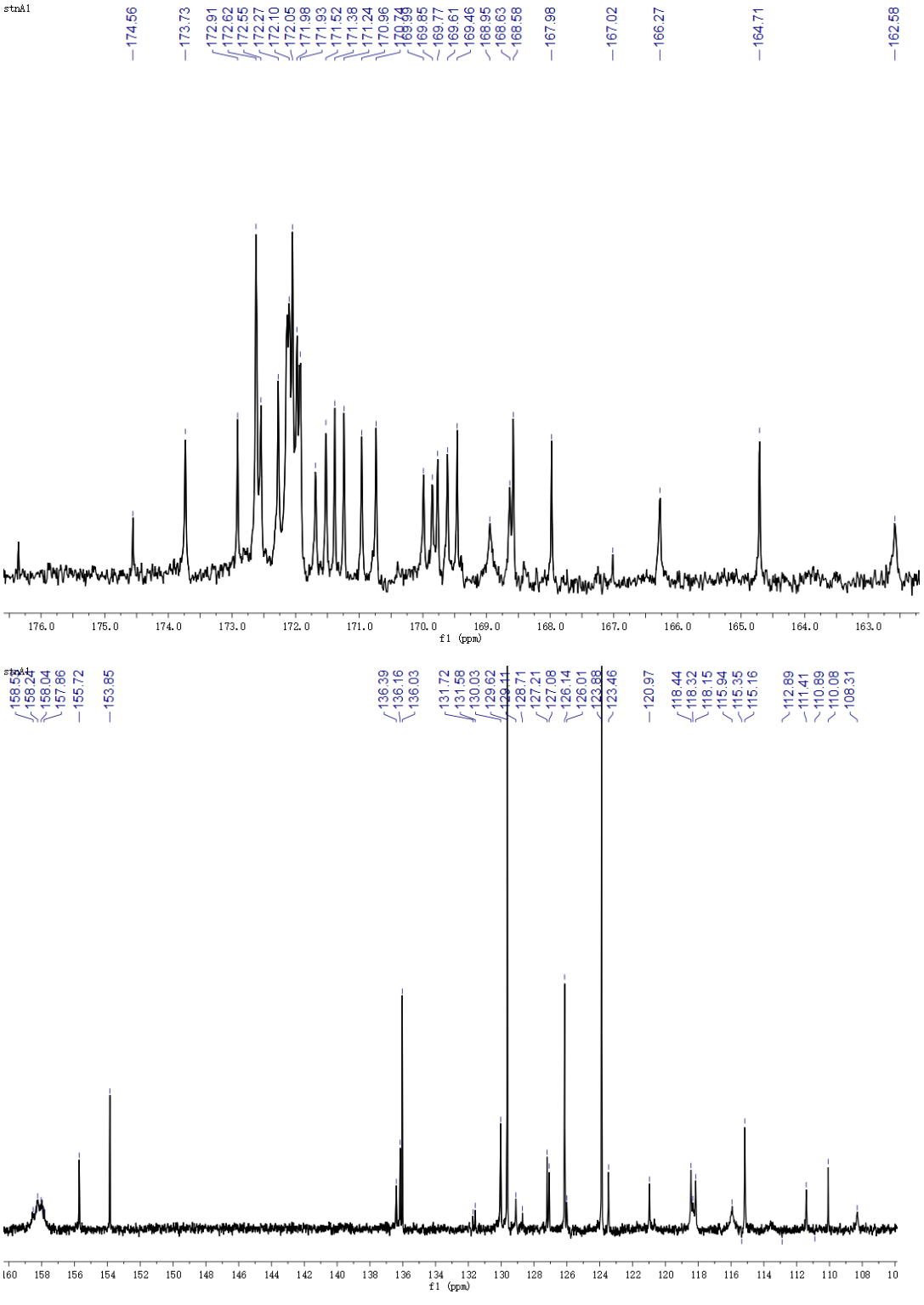

(iv), Localized zoom-in of ^{13}C NMR spectrum of **1** in DMSO-d_6.

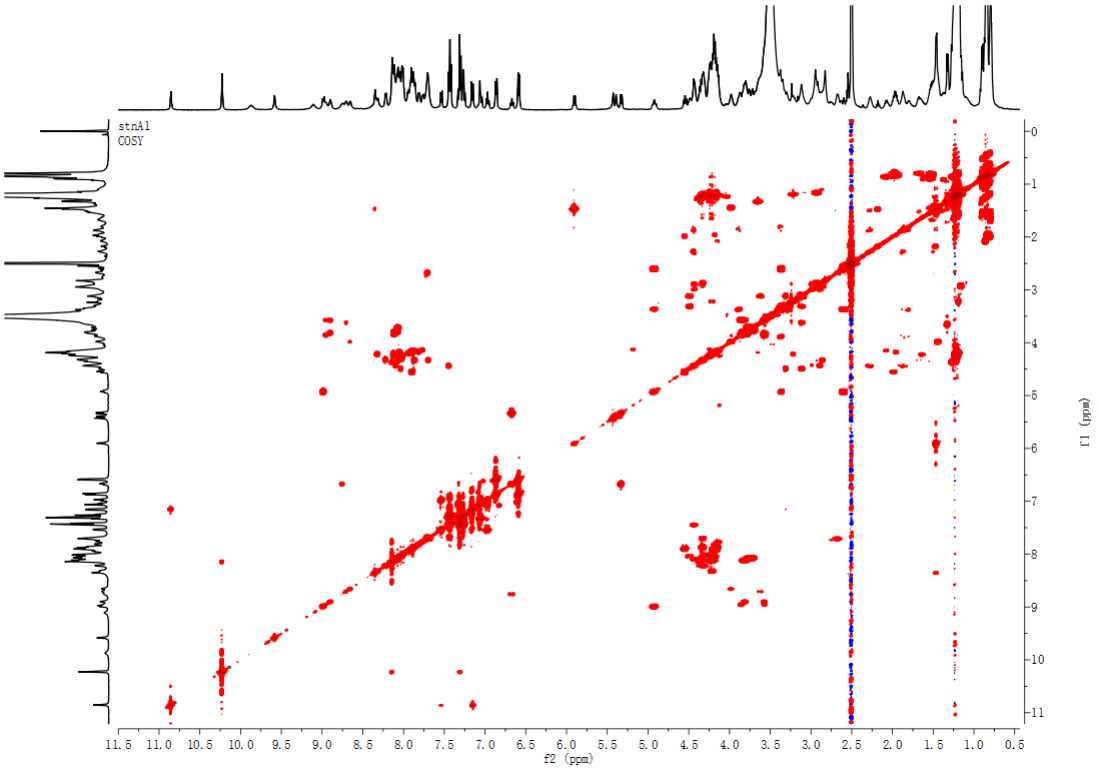

(v), ^{1}H-^{1}H COSY spectrum of **1** in DMSO-d_6.

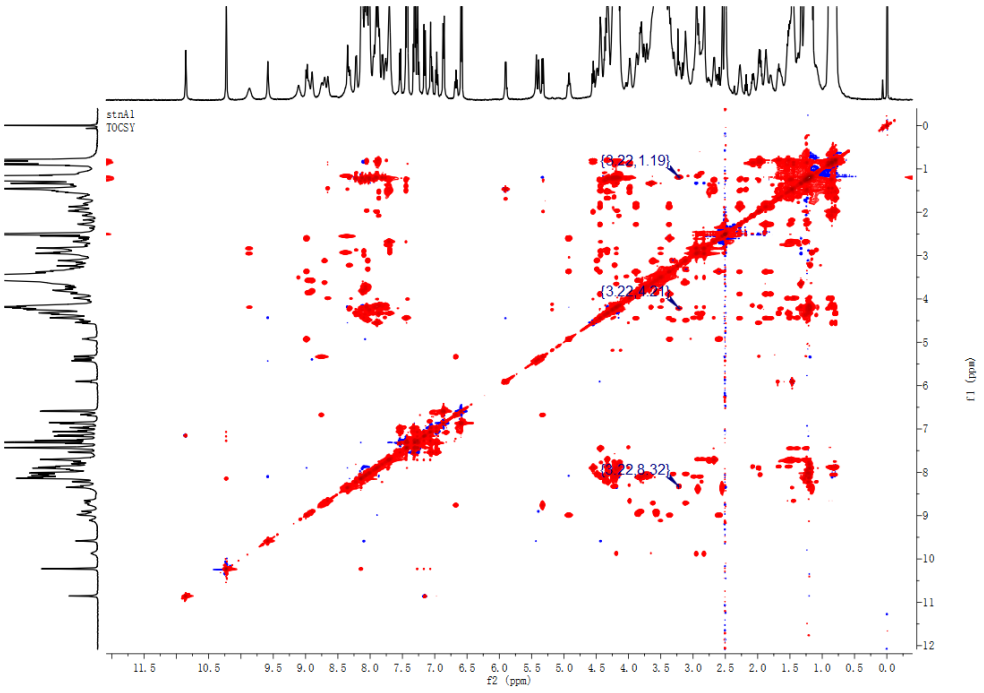

(vi), TOCSY spectrum of **1** in DMSO-d_6.

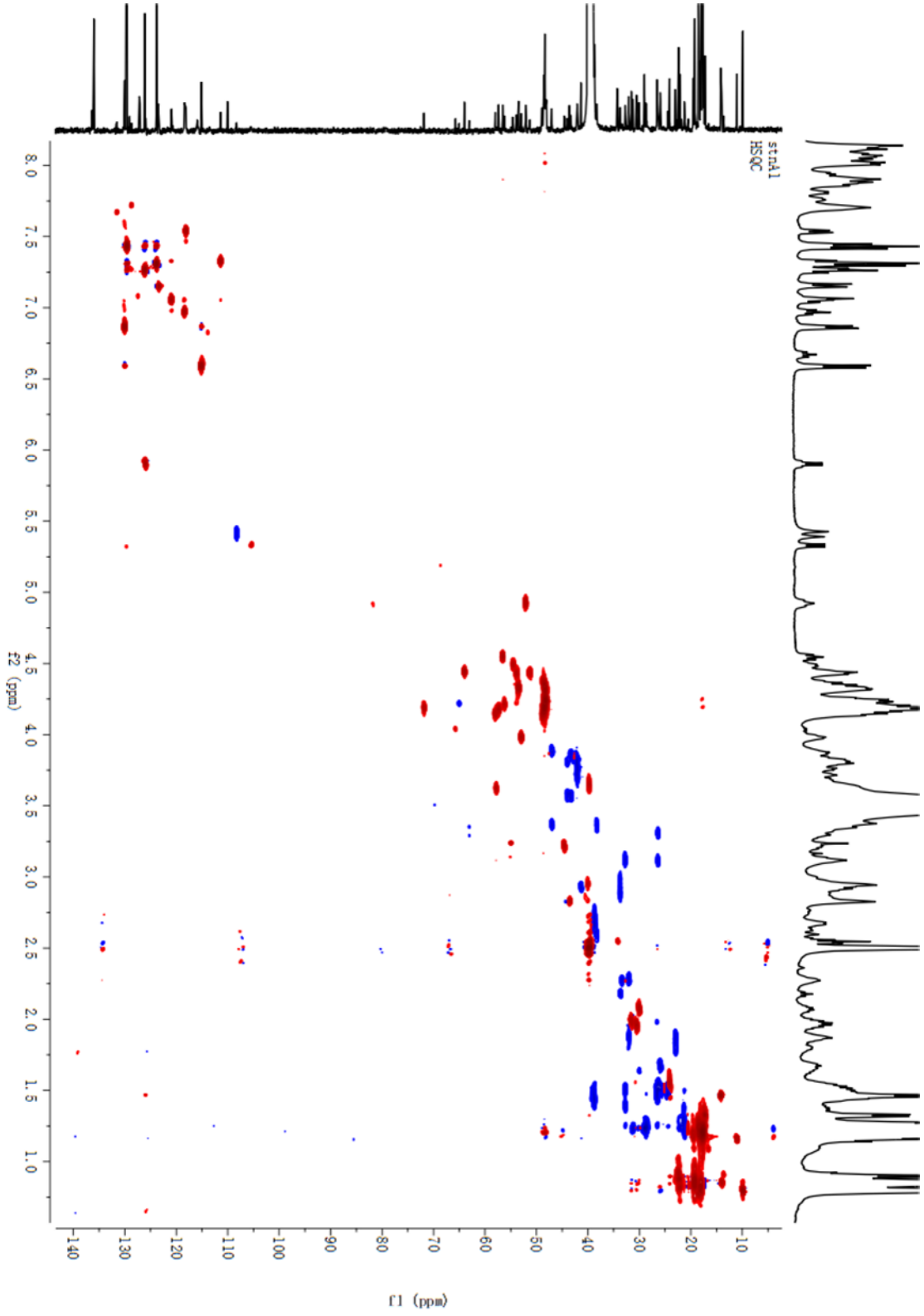

(vii), HSQC spectrum of **1** in DMSO-d_6.

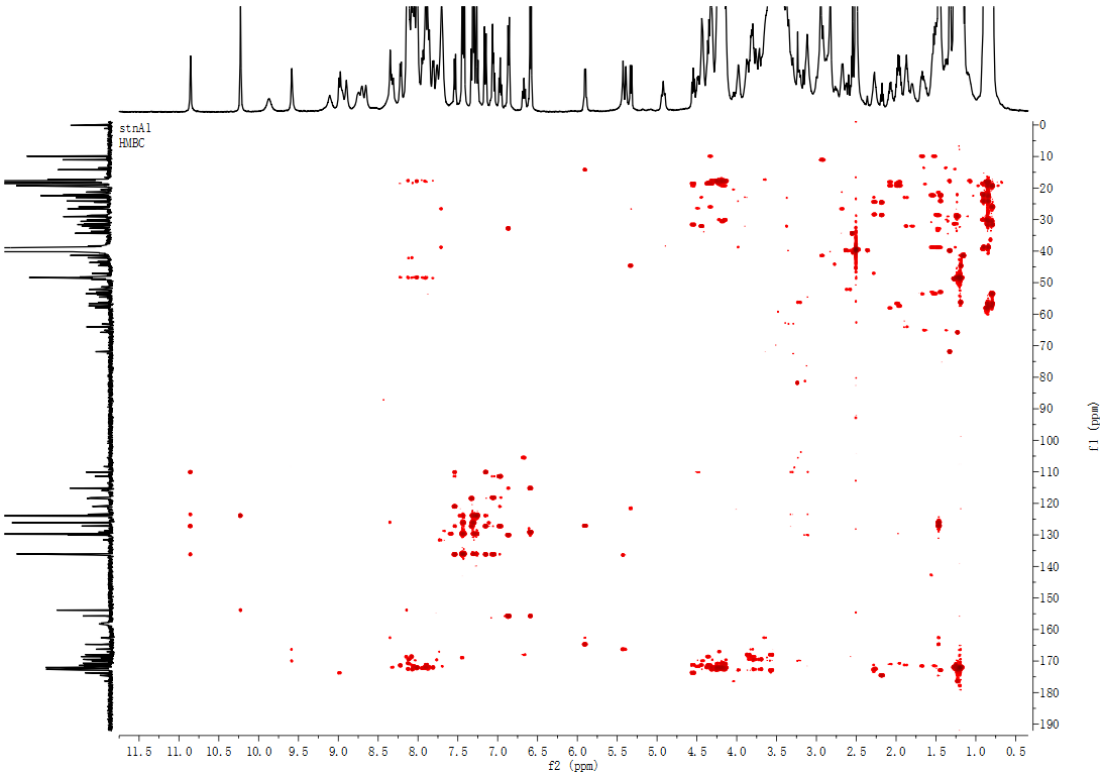

(viii), HMBC spectrum of **1** in DMSO-d_6.

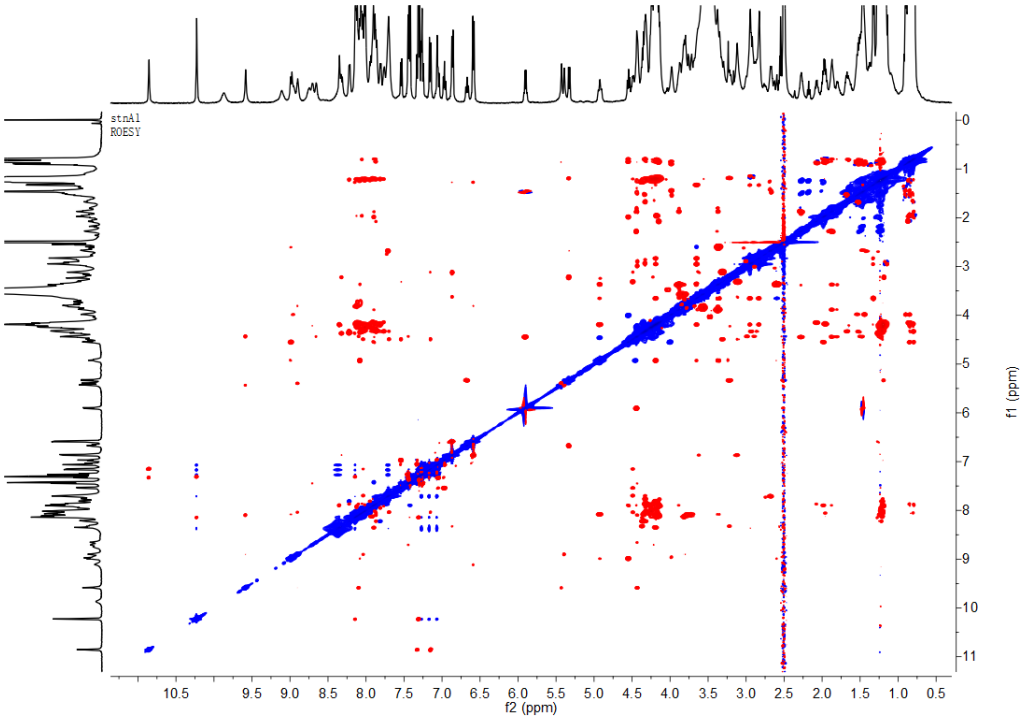

(ix), ROESY spectrum of **1** in DMSO-d_6.

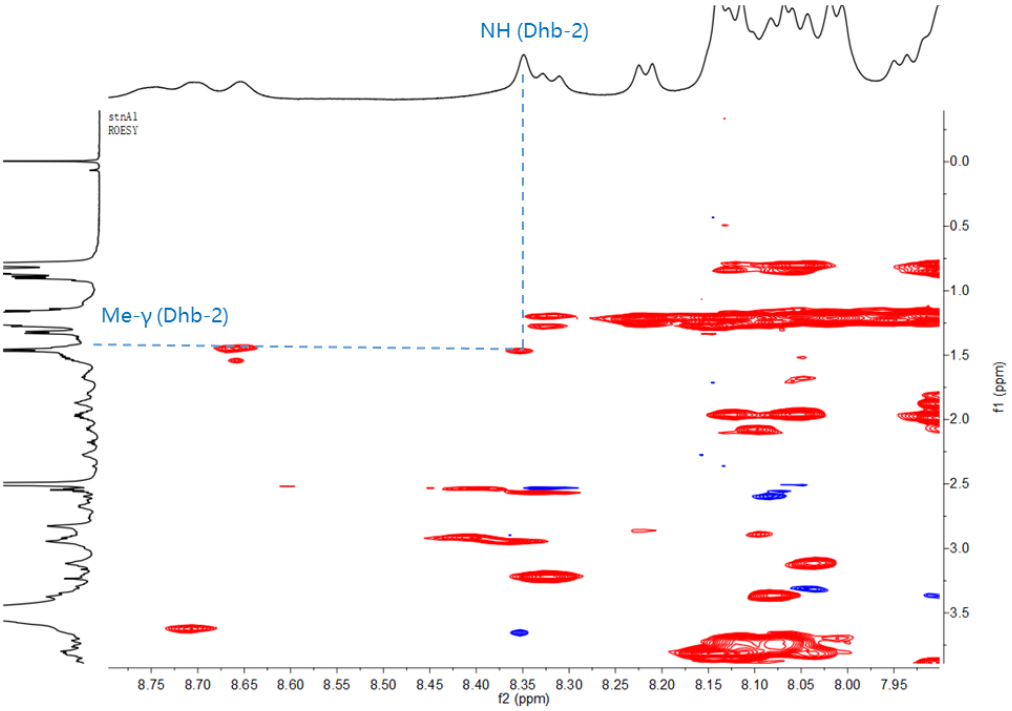

(x), Localized zoom-in of ROESY spectrum of the Dhb-2 fragment in **1**.

Figure. S8. NMR spectra of **1**.

(A), Key 2D correlations of **3**.

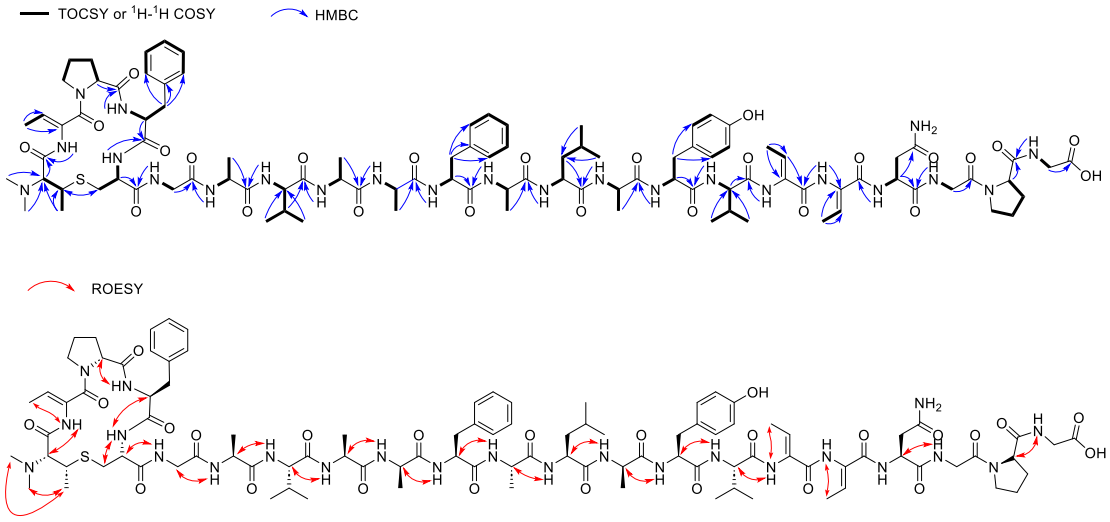

(B), 1D and 2D NMR spectra of **3** in DMSO-d_6.

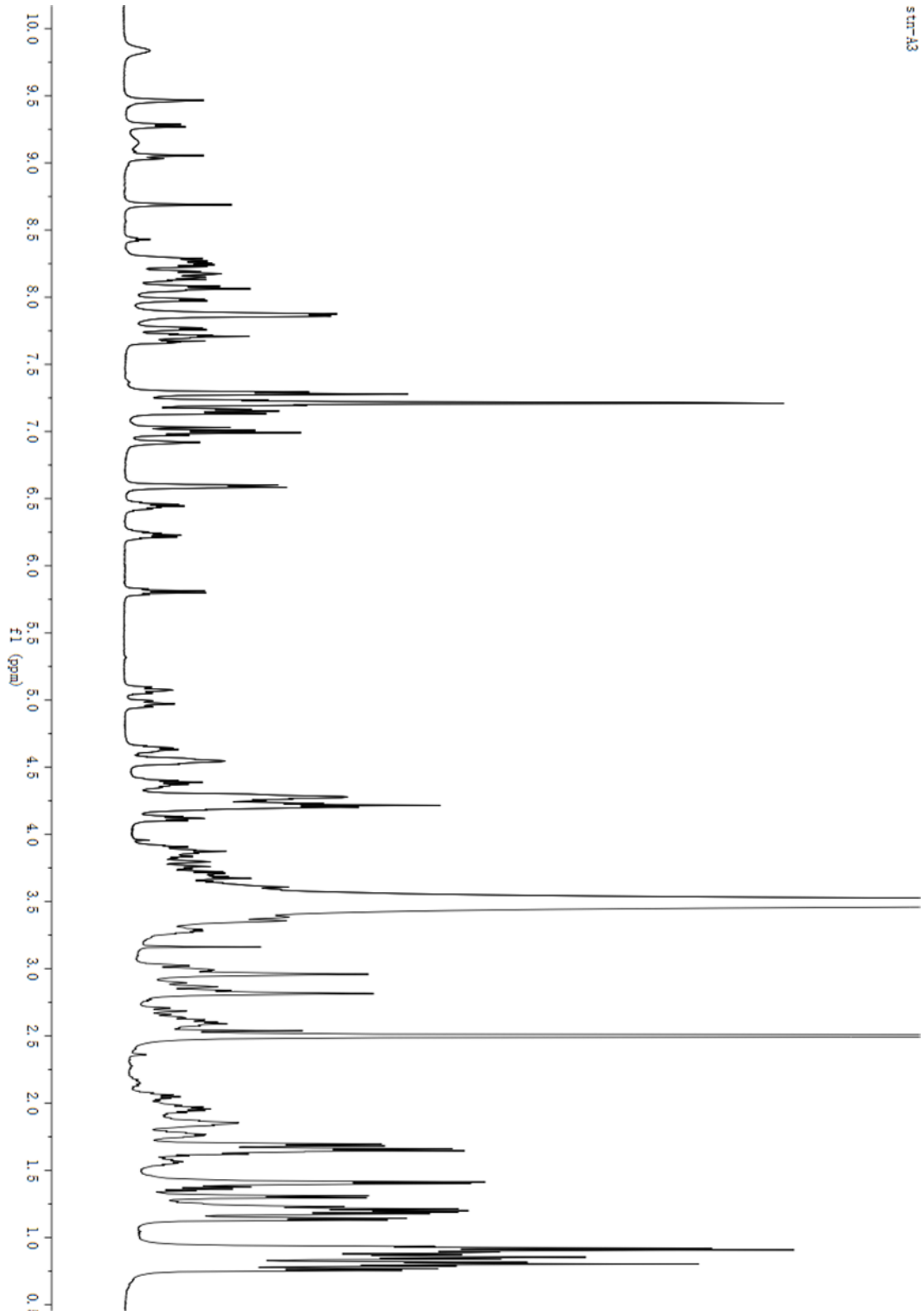

(i), ^{1}H NMR spectrum (full spectrum) of **3** in DMSO-d_6.

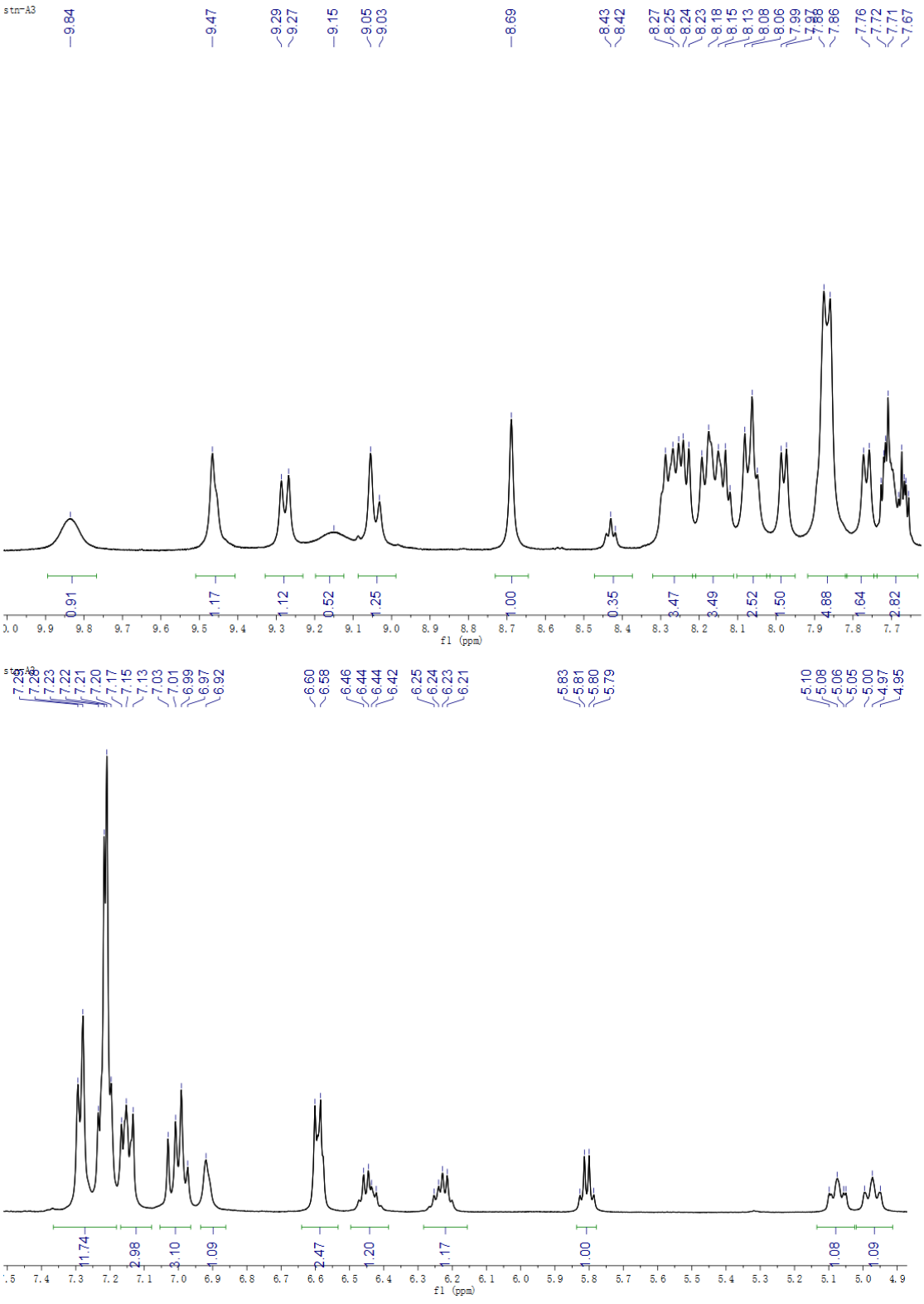

(ii), Localized zoom-in of ^{1}H NMR spectrum of **3** in DMSO-d_6.

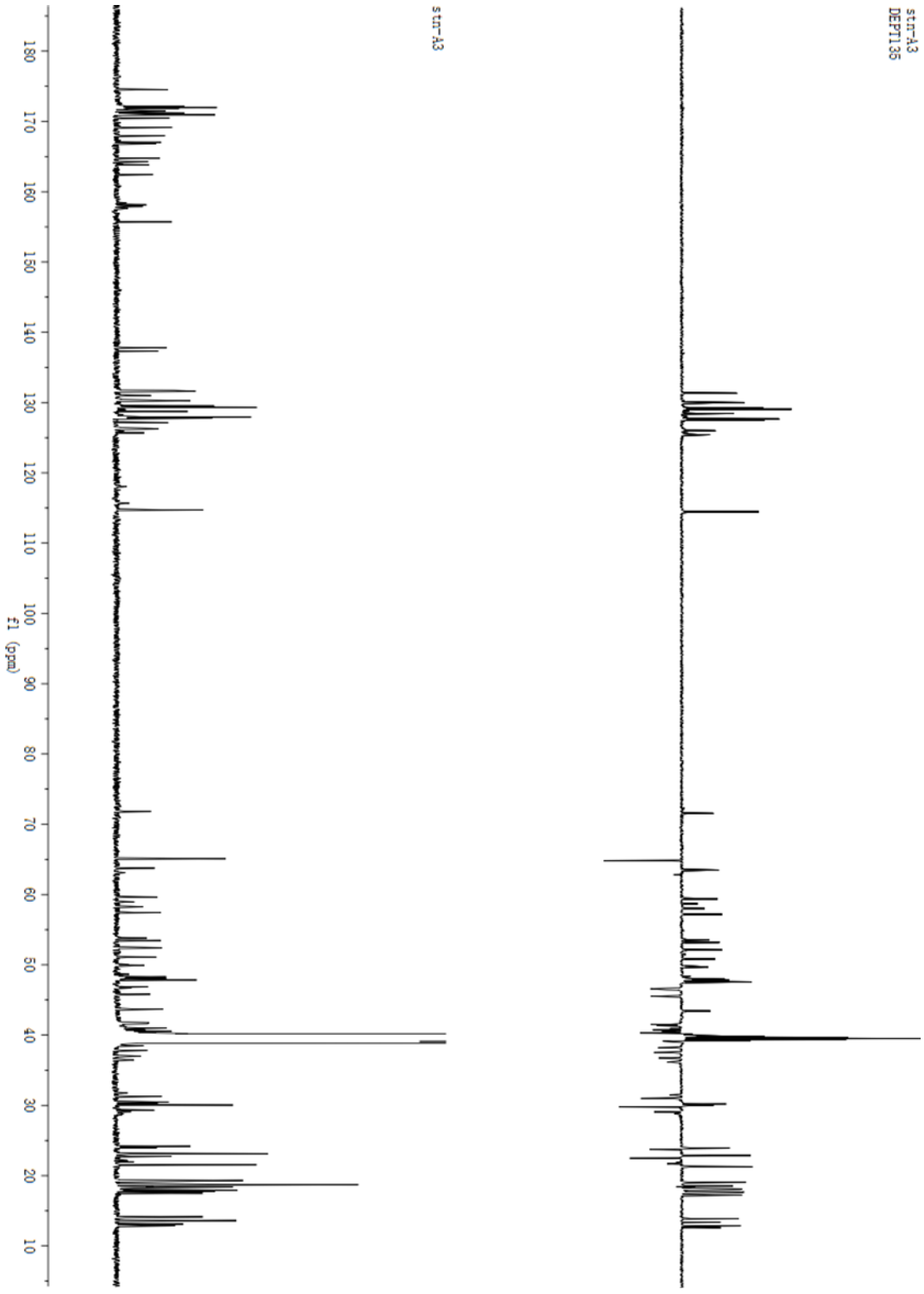

(iii), ^{13}C NMR spectrum (full spectrum) of **3** in DMSO-d_6.

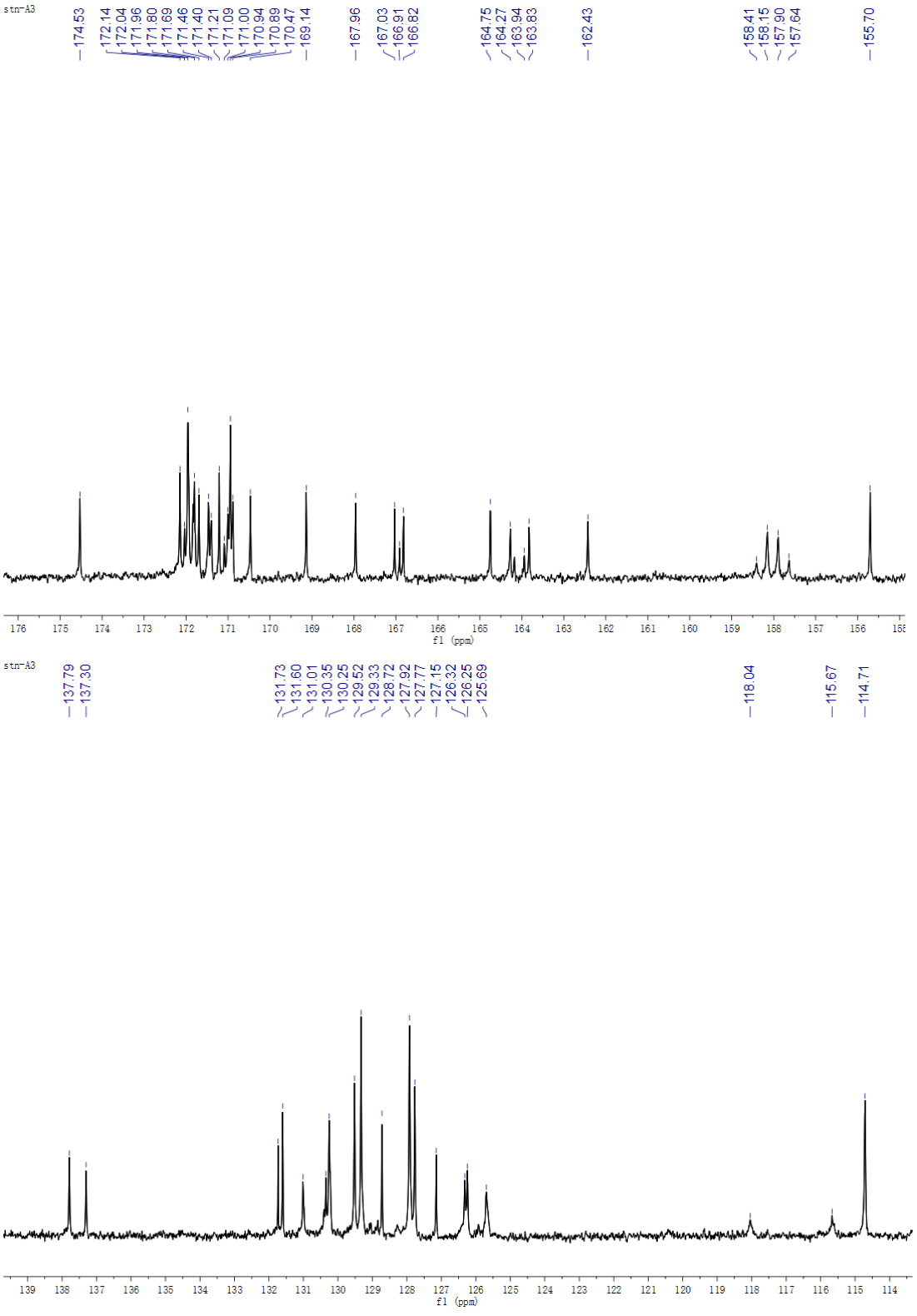

(iv), Localized zoom-in of ^{13}C NMR spectrum of **3** in DMSO-d_6.

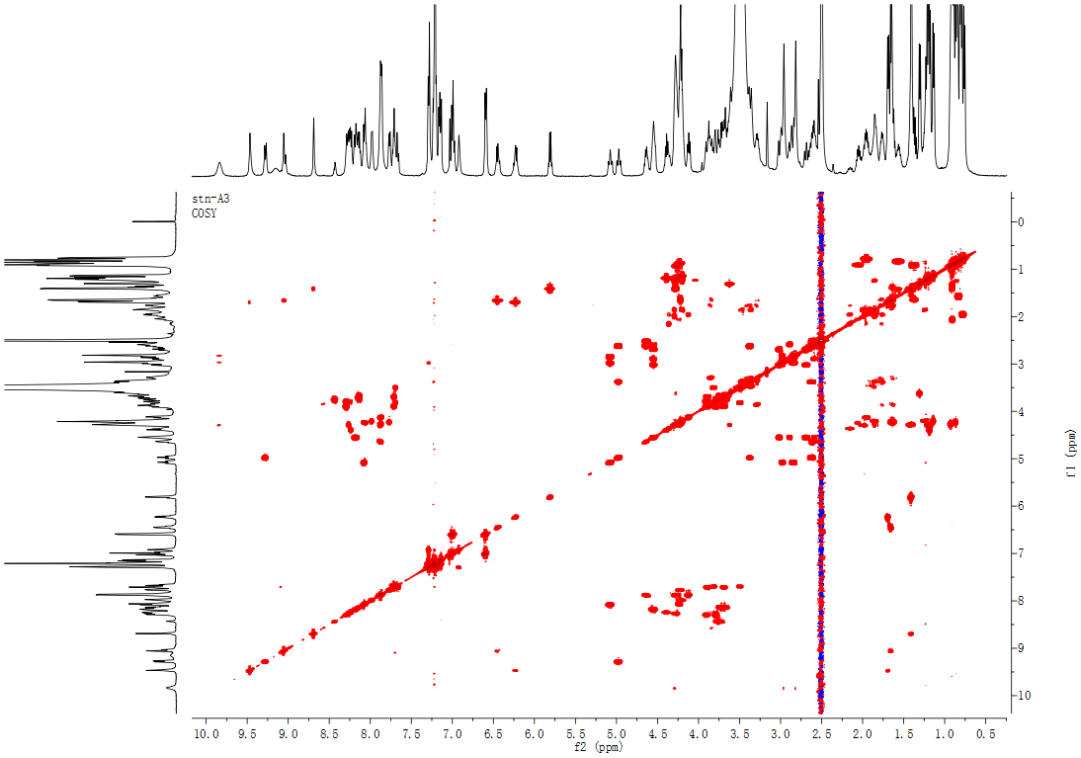

(v), ^{1}H-^{1}H COSY spectrum of **3** in DMSO-d_6.

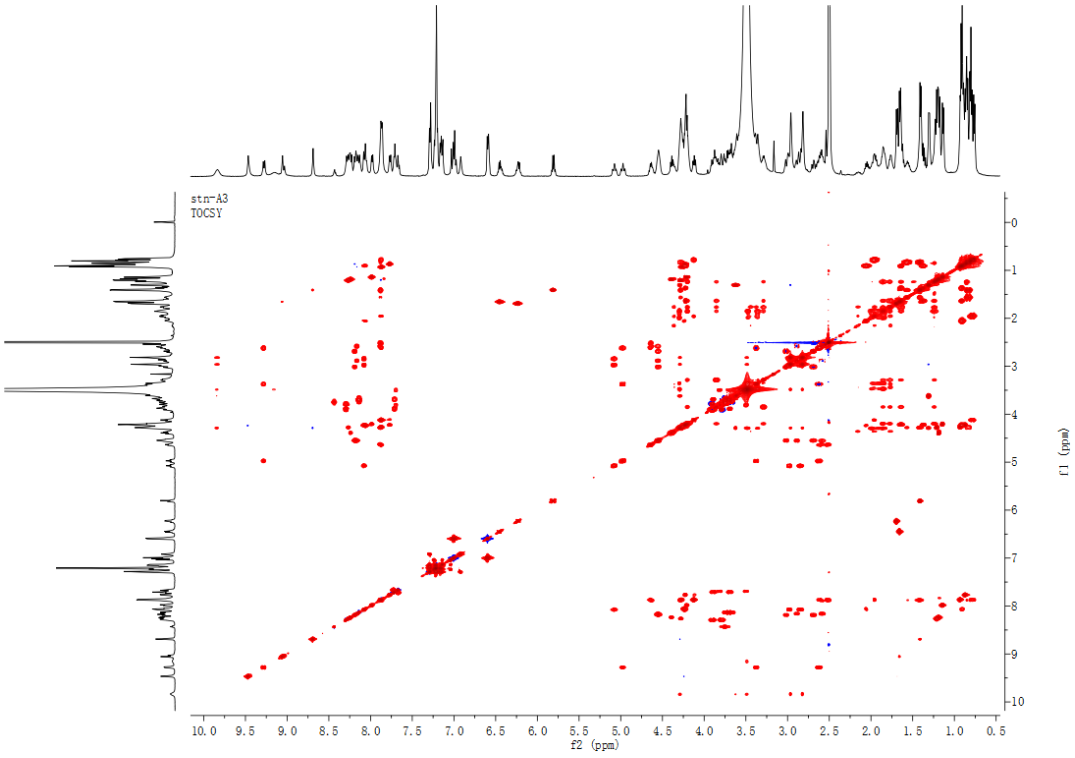

(vi), TOCSY spectrum of **3** in DMSO-d_6.

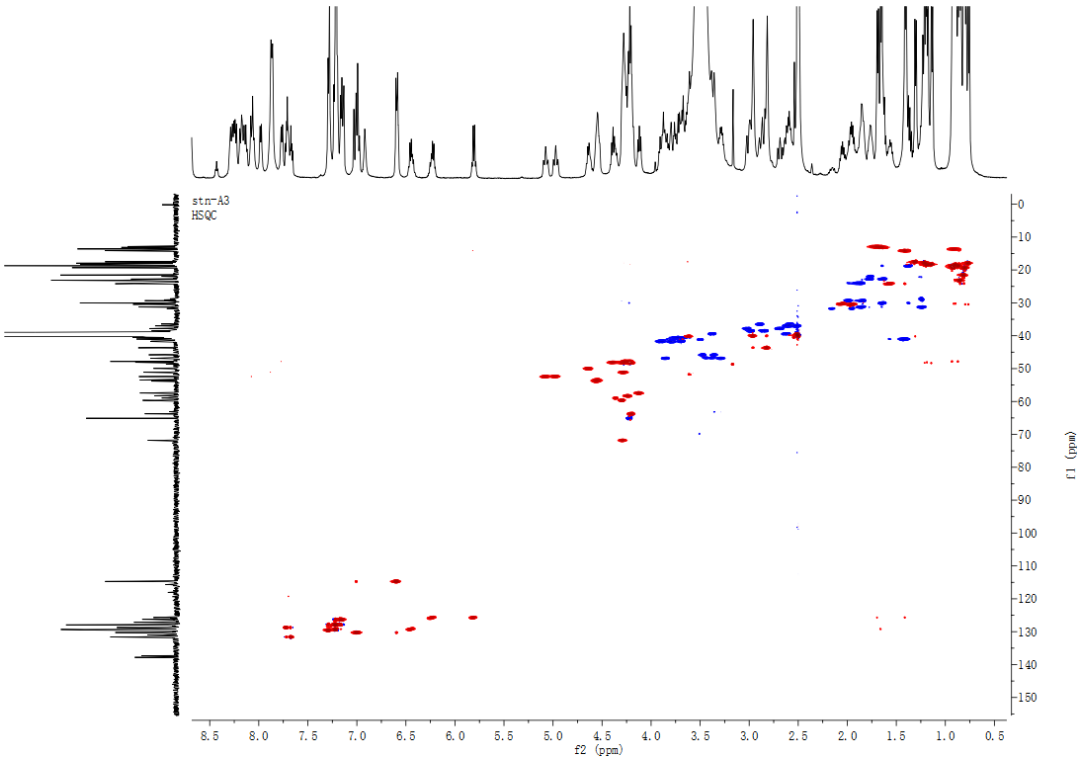

(vii), HSQC spectrum of **3** in DMSO-d_6.

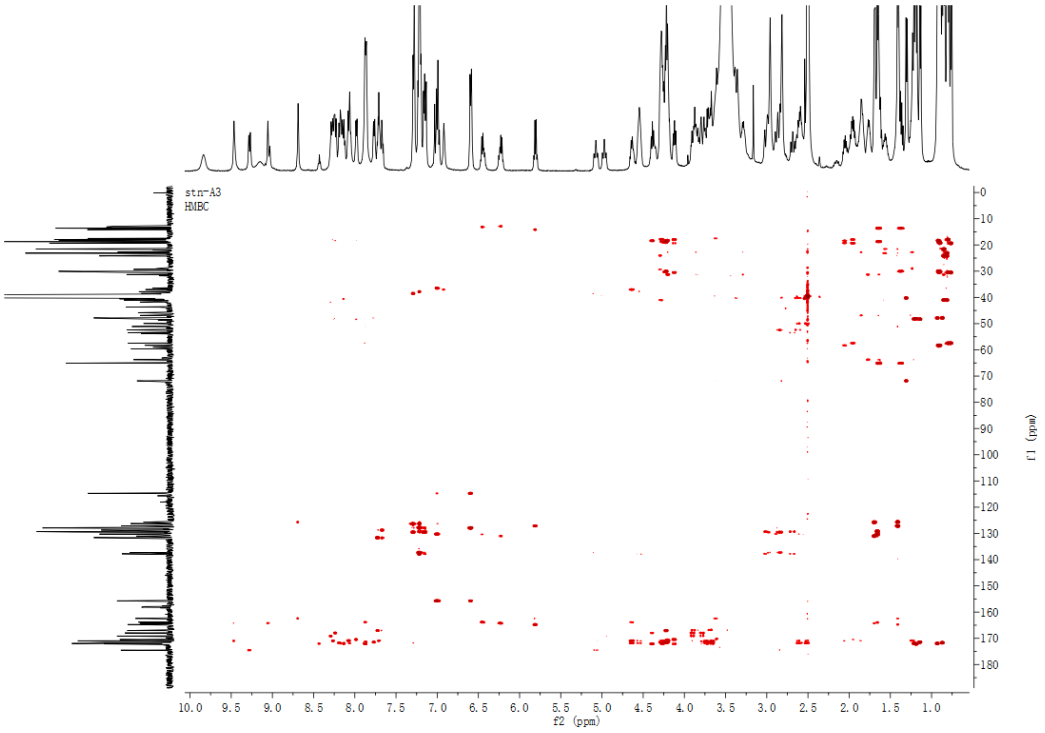

(viii), HMBC spectrum of **3** in DMSO-d_6.

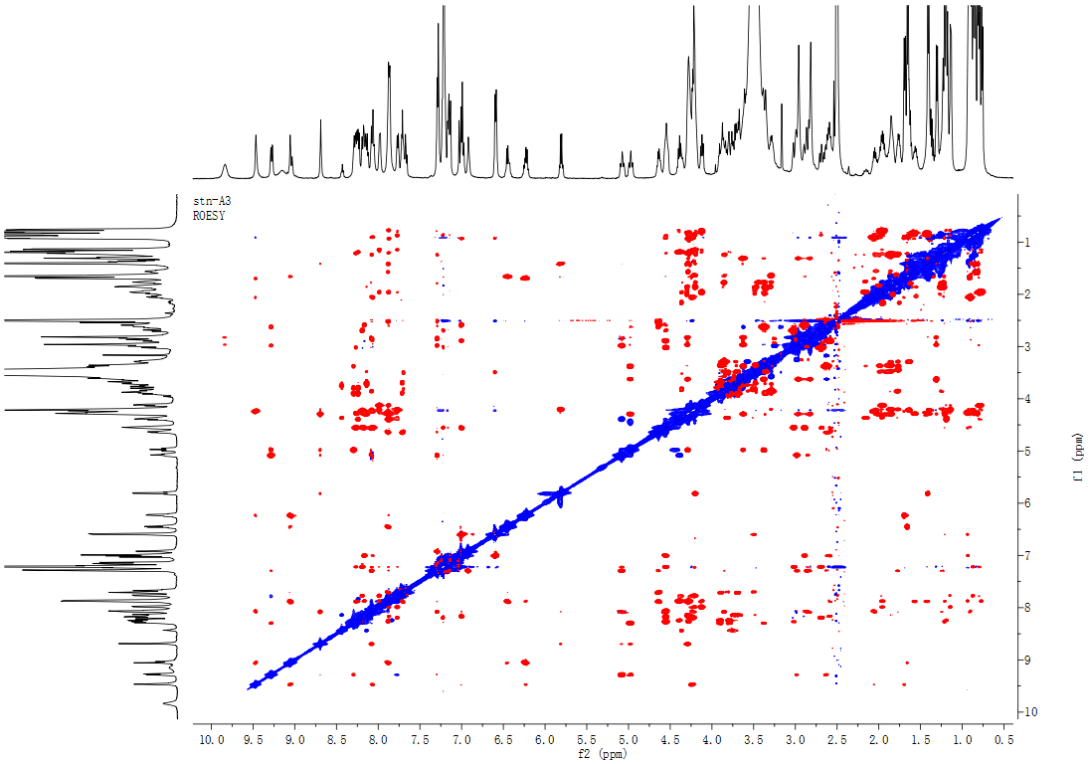

(ix), ROESY spectrum of **3** in DMSO-d_6.

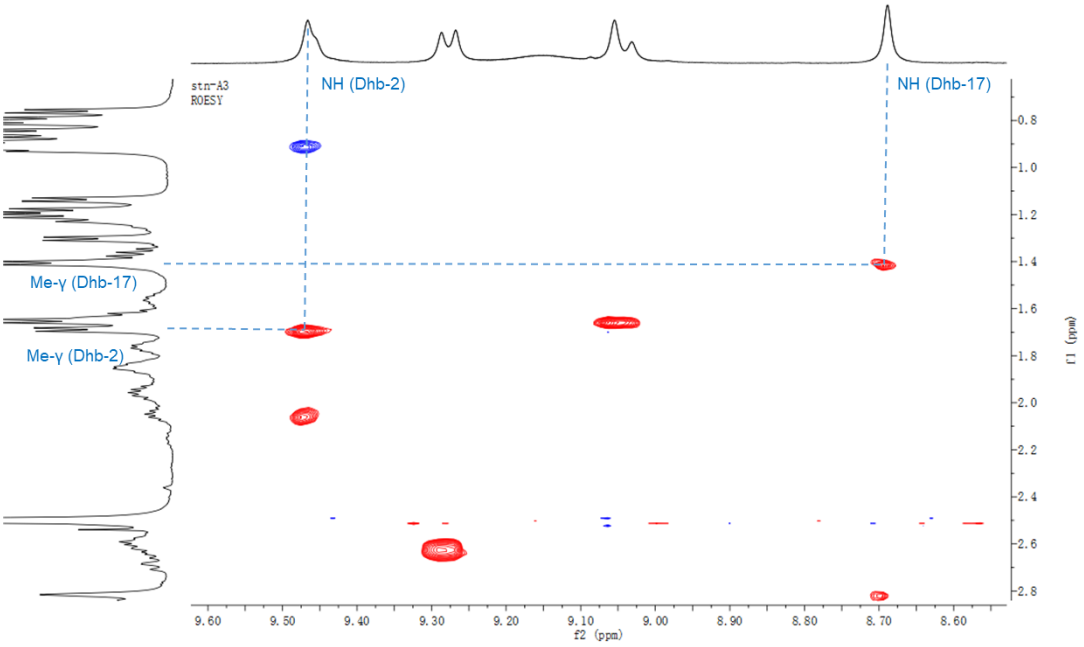

(x), Localized zoom-in of ROESY spectrum of the Dhb-2 and Dhb-17 fragments in **3**.

Figure. S9. NMR spectra of **3**.

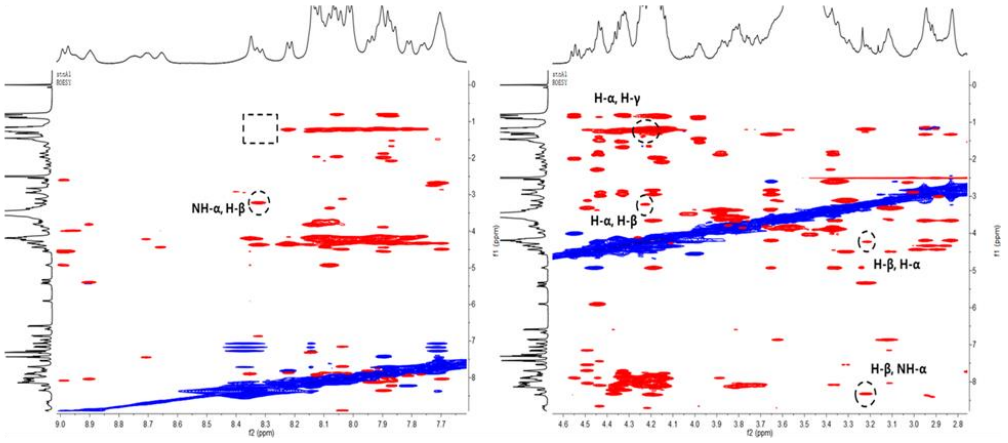

Figure S10. Determination of AviMeCys stereochemistry using ^{1}H-^{1}H ROESY. Localized zoom-in of ROESY spectrum of the AviMeCys fragment in **1** is shown.

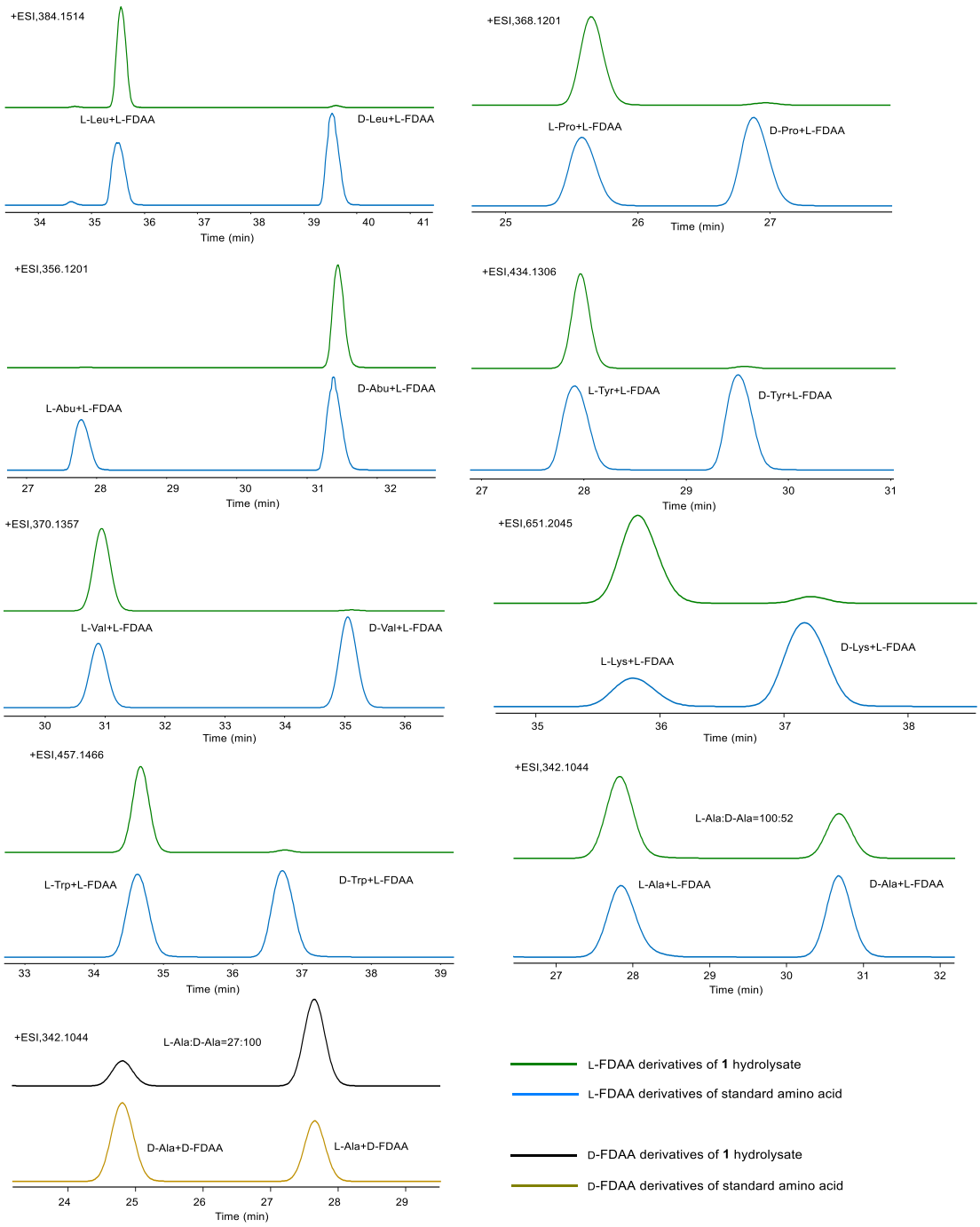

Figure. S11. Chiral analysis of residues in **1**. The peak area ratio of L-FDAA-L-Ala / L-FDAA-D-Ala is not proportional, while the peak area ratio of D-FDAA-L-Ala / D-FDAA-D-Ala (100/27) is close to the ratio of 12 L-Ala / 3 D-Ala. The 3 newly generated Ala residues from former Ser residues were tentatively assigned in D-configuration.

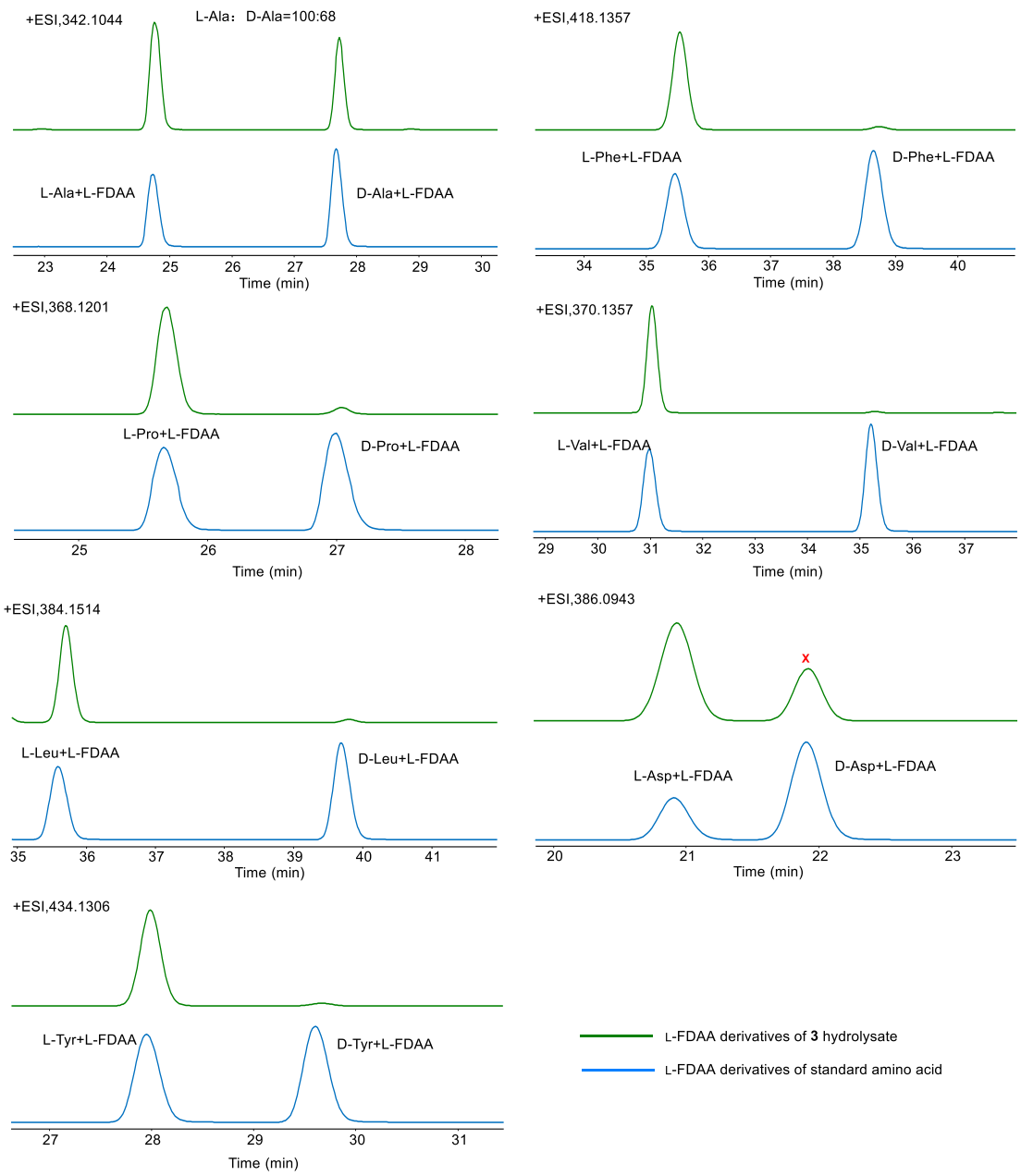

Figure. S12. Chiral analysis of residues in **3**. The peak area ratio of L-FDAA-L-Ala / L-FDAA-D-Ala is 100:68, which is close to the ratio of 3 L-Ala / 2 D-Ala. The 2 newly generated Ala residues from former Ser residues were tentatively assigned in D-configuration.

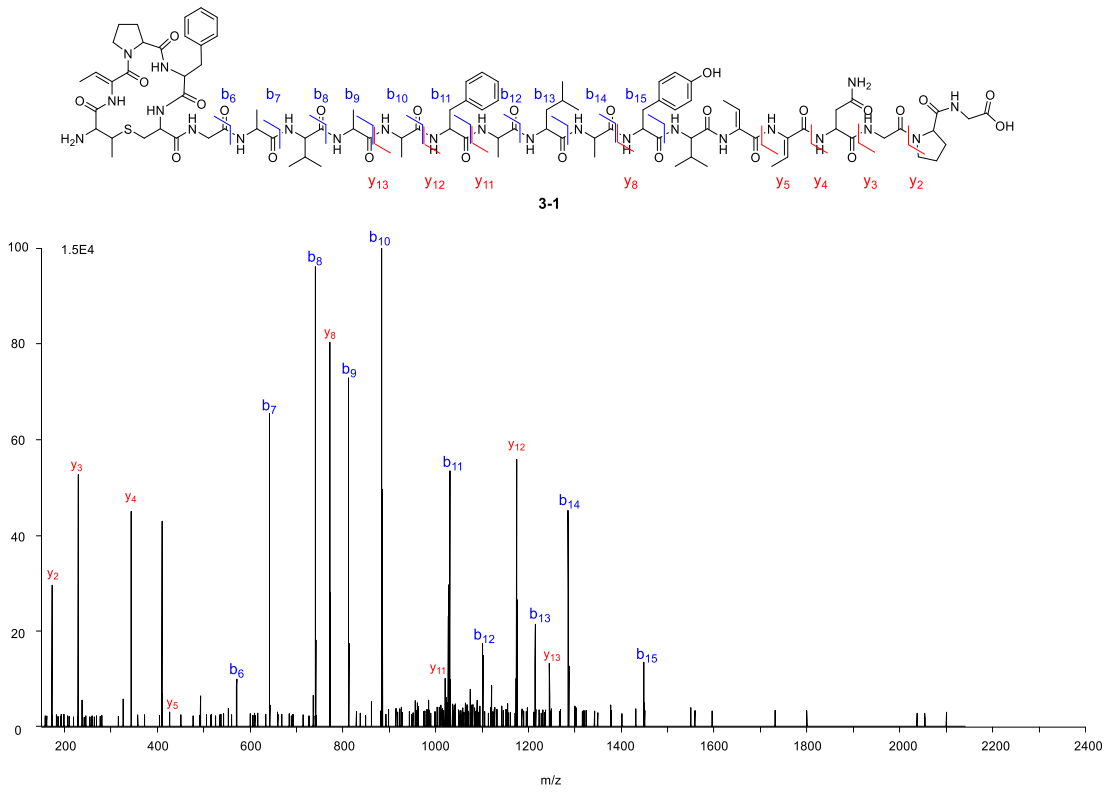

Ions	Calc.	Obs.	Er.(ppm)	Ions	Calc.	Obs.	Er.(ppm)
b6	571.2245	571.2259	2.5	**y13**	1245.6071	1245.6167	7.7
b7	642.2617	642.2657	6.2	**y12**	1174.5746	1174.5834	7.5
b8	741.3300	741.3308	1.1	**y11**	1027.5062	1027.5139	7.5
b9	812.3671	812.3698	3.3	**y8**	772.3525	772.3540	1.9
b10	883.3997	883.4048	5.8	**y5**	427.1884	427.1844	9.4
b11	1030.4680	1030.4770	8.7	**y4**	344.1559	344.1572	3.8
b12	1101.5051	1101.5096	4.1	**y3**	230.1130	230.1140	4.3
b13	1214.5892	1214.596	5.6	**y2**	173.0915	173.0925	5.8
b14	1285.6217	1285.6281	5.0				
b15	1448.6851	1448.6948	6.7				

Figure. S13. MS analysis of **3-1**. The HCD fragments and the MS/MS spectrum are shown.

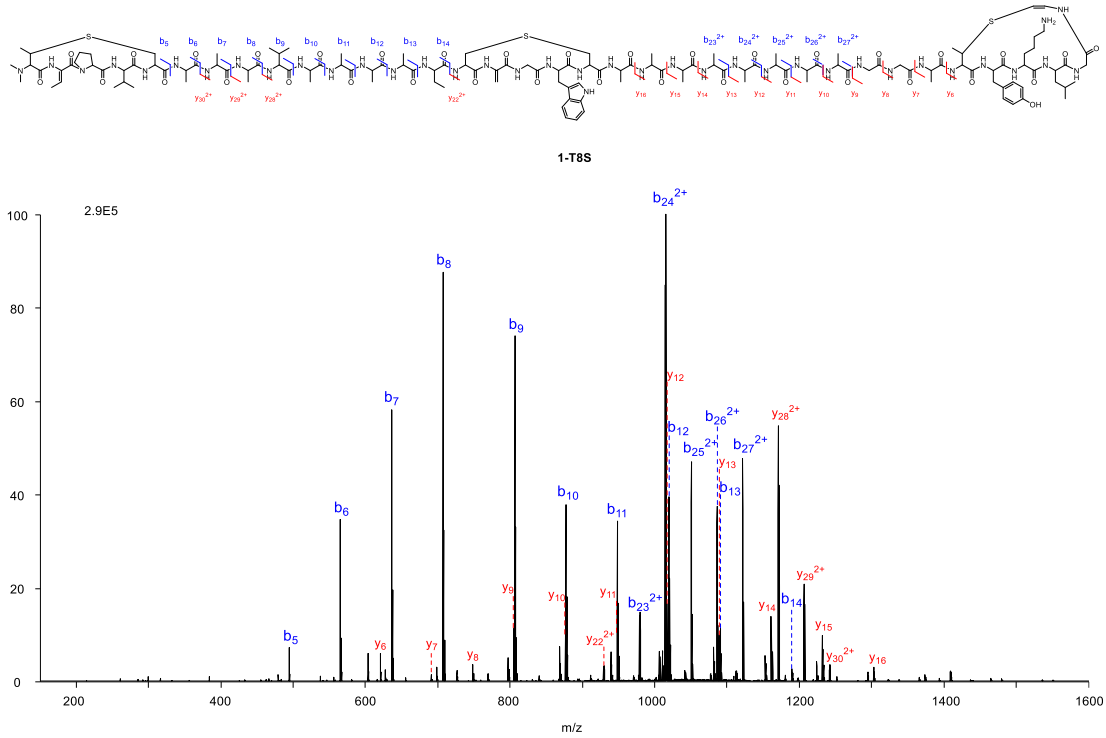

Ions	Calc.	Obs.	Er.(ppm)	Ions	Calc.	Obs.	Er.(ppm)
b5	494.2343	494.24	11.5	**y16**	1302.6571	1302.6664	7.1
b6	565.2715	565.2765	8.8	**y15**	1231.6200	1231.6279	6.4
b7	636.3086	636.3145	9.3	**y14**	1160.5829	1160.5898	5.9
b8	707.3457	707.3526	9.8	**y13**	1089.5458	1089.5538	7.3
b9	806.4141	806.4235	11.7	**y12**	1018.5086	1018.5155	6.8
b10	877.4512	877.4599	9.9	**y11**	947.4715	947.4782	7.1
b11	948.4883	948.4916	3.5	**y10**	876.4344	876.4403	6.7
b12	1019.5255	1019.534	8.3	**y9**	805.3973	805.4035	7.7
b13	1090.5625	1090.5648	2.1	**y8**	748.3758	748.382	8.3
b14	1189.6310	1189.6401	7.6	**y7**	691.3544	691.3604	8.7
$b23^{2+}$	979.4651	979.4674	2.3	**y6**	620.3173	620.3234	9.8
$b24^{2+}$	1014.9837	1014.986	2.3	**$y30^{2+}$**	1241.6023	1241.6121	7.9
$b25^{2+}$	1050.5022	1050.505	2.7	**$y29^{2+}$**	1206.0837	1206.0932	7.9
$b26^{2+}$	1086.0208	1086.023	2.0	**$y28^{2+}$**	1170.5652	1170.5745	7.9
$b27^{2+}$	1121.5393	1121.5413	1.8	**$y22^{2+}$**	929.4225	929.4302	8.3

Figure. S14. MS analysis of **1-T8S**. The HCD fragments and the MS/MS spectrum are shown.

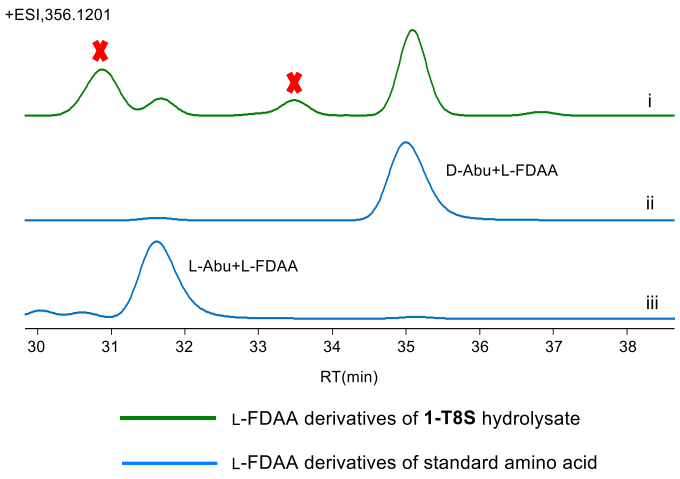

Figure. S15. Chiral analysis of aminobutyric acid residues in **1-T8S**. L-FDAA derivatives of aminobutyric acid (Abu) residue in **1-T8S** hydrolysate (i), D-Abu standard (ii), and L-Abu standard (iii).

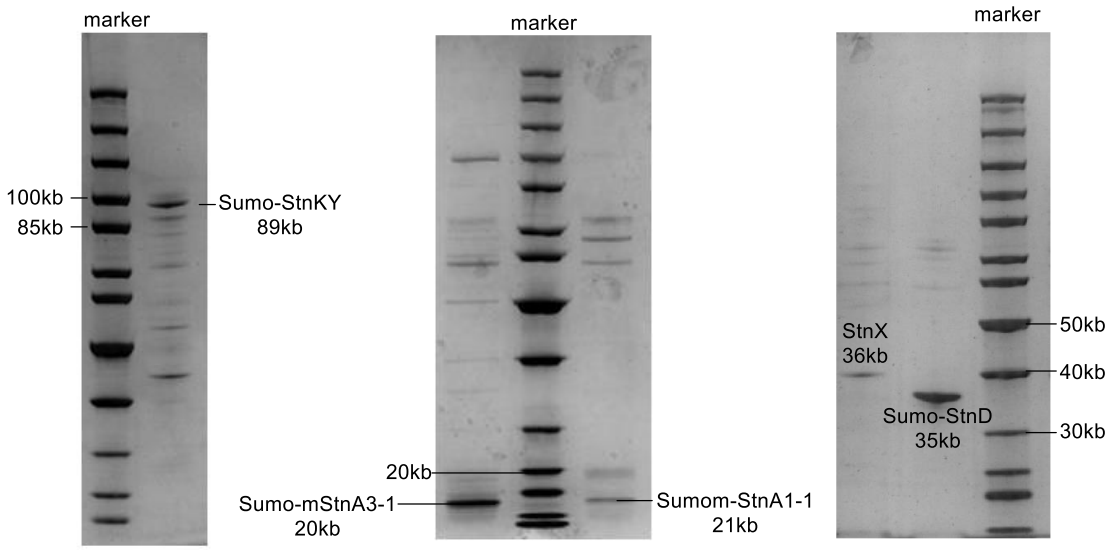

Figure. S16. SDS-PAGE analysis of engineered proteins.

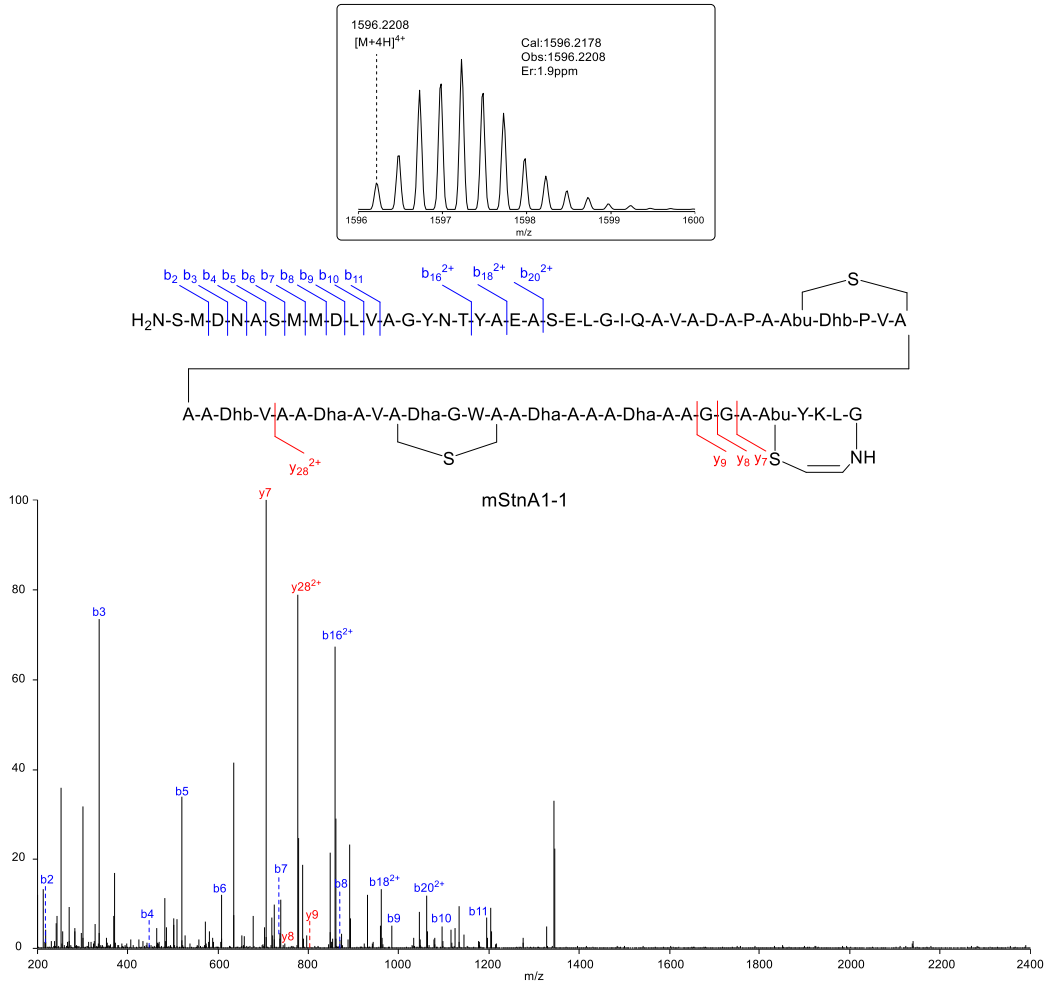

Ions	Calc.	Obs.	Er.(ppm)	Ions	Calc.	Obs.	Er.(ppm)
b2	219.0803	219.0813	4.5	**y9**	805.3973	805.3951	2.7
b3	334.1073	334.1085	3.6	**y8**	748.3758	748.3742	2.1
b4	448.1502	448.1524	4.9	**y7**	691.3544	691.3535	1.3
b5	519.1873	519.1844	5.6	**$y28^{2+}$**	1167.5347	1167.533	1.5
b6	606.2194	606.2177	2.8				
b7	737.2598	737.2583	2.0				
b8	868.3003	868.3015	1.4				
b9	983.3273	983.3289	1.6				
b10	1096.4113	1096.4101	1.1				
b11	1195.4797	1195.4769	2.3				
$b16^{2+}$	851.3498	851.348	2.1				
$b18^{2+}$	968.4000	968.392	8.3				
$b20^{2+}$	1068.4398	1068.4368	2.8				

Figure. S17. MS analysis of mStnA1-1. The HR-MS, HCD fragments, and the MS/MS spectrum are shown.

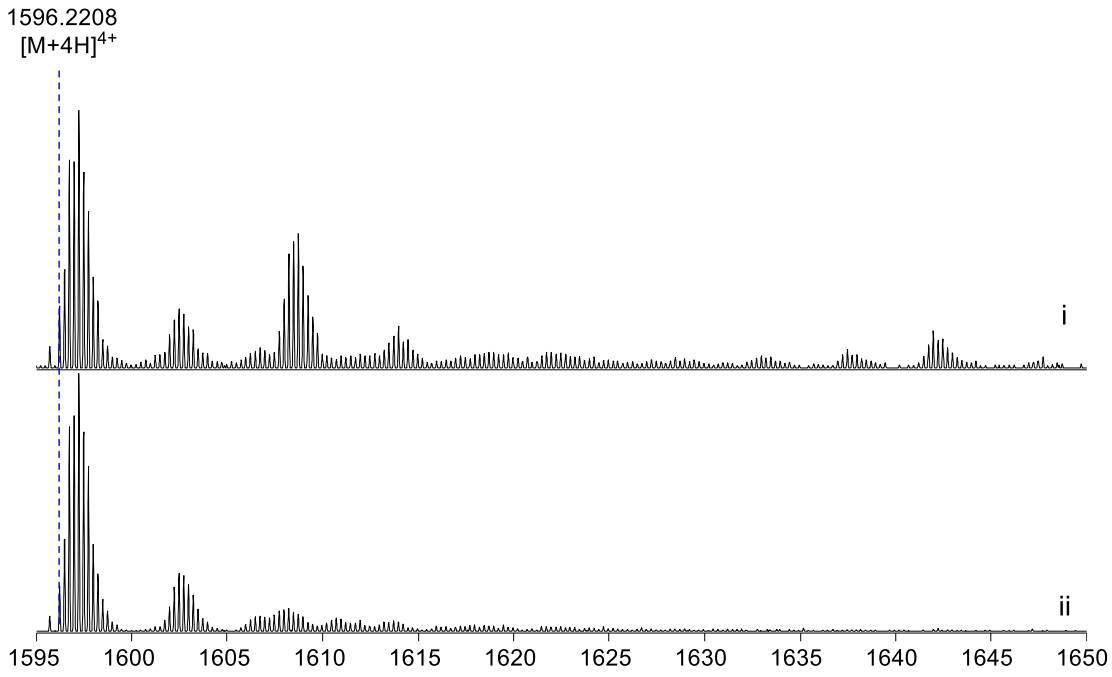

Figure. S18. Iodoacetamide derivatization of mStnA1-1. mStnA1-1(i), and mStnA1-1 + iodoacetamide (ii). The calculated $[M+4H]^{4+}$ for mStnA1-1 is 1596.2178.

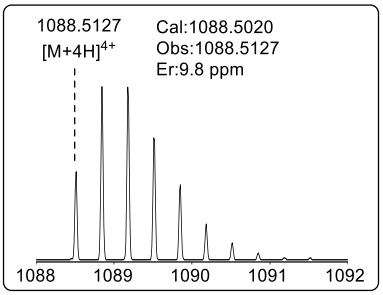
1088.5127
[M+4H]4+
Cal:1088.5020
Obs:1088.5127
Er:9.8 ppm
1088
1089
1090
1091
1092

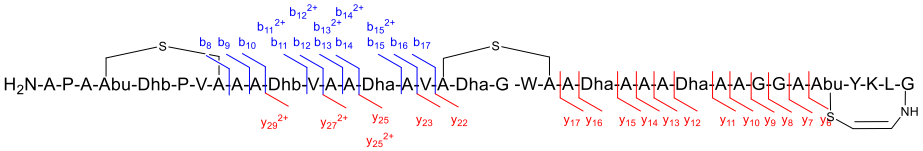
H2N-A-P-A-Abu-Dhb-P-V-A-A-A-Dhb-V-A-A-Dha-A-V-A-Dha-G -W-A-A-Dha-A-A-A-Dha-A-A-G-G-A-Abu-Y-K-L-G
S
S
S
NH

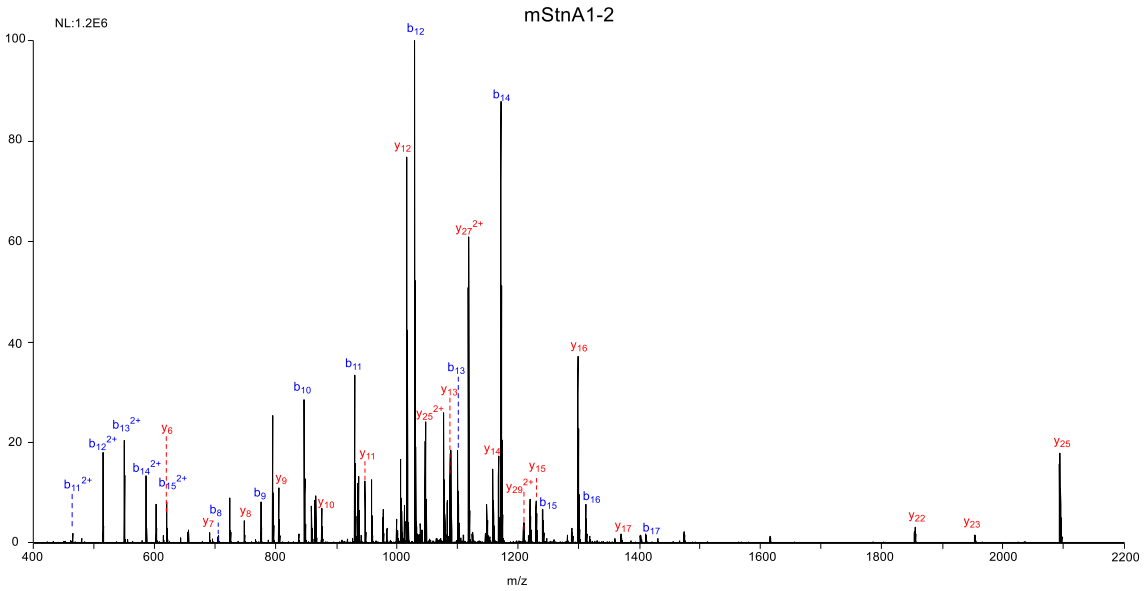
mStnA1-2
NL:1.2E6
m/z
100
80
60
40
20
0
400
600
800
1000
1200
1400
1600
1800
2000
2200

Ions	Calc.	Obs.	Er.(ppm)	Ions	Calc.	Obs.	Er.(ppm)
b8	705.3300	705.3358	8.2	**y25**	2092.9194	2092.9251	2.7
b9	776.3671	776.3728	7.3	**y23**	1952.8655	1952.8685	1.5
b10	847.4042	847.4103	7.2	**y22**	1853.7970	1853.792	2.7
b11	930.4367	930.4472	11.3	**y17**	1369.6536	1369.6586	3.7
b12	1029.5051	1029.5129	7.6	**y16**	1298.6165	1298.6195	2.3
b13	1100.5422	1100.5523	9.2	**y15**	1229.5996	1229.5920	6.2
b14	1171.5793	1171.5863	6.0	**y14**	1158.5625	1158.5600	2.2
b15	1240.5961	1240.5943	1.5	**y13**	1087.5254	1087.5201	4.9
b16	1311.6332	1311.6204	9.8	**y12**	1016.4883	1016.4821	6.1
b17	1410.7017	1410.7082	4.6	**y11**	947.4715	947.4767	5.5
$b11^{2+}$	465.7220	465.7266	9.9	**y10**	876.4344	876.4395	5.8
$b12^{2+}$	515.2562	515.2609	9.1	**y9**	805.3973	805.4005	4.0
$b13^{2+}$	550.7748	550.7781	6.0	**y8**	748.3758	748.3791	4.4
$b14^{2+}$	586.2933	586.2969	6.1	**y7**	691.3544	691.3596	7.5
$b15^{2+}$	620.8017	620.8063	7.4	**y6**	620.3173	620.3123	8.1
				$y29^{2+}$	1209.0509	1209.0539	2.5
				$y27^{2+}$	1118.0005	1118.0068	5.6
				$y25^{2+}$	1046.9634	1046.9669	3.3

Figure. S19. MS analysis of mStnA1-2. The HR-MS, HCD fragments, and the MS/MS spectrum are shown.

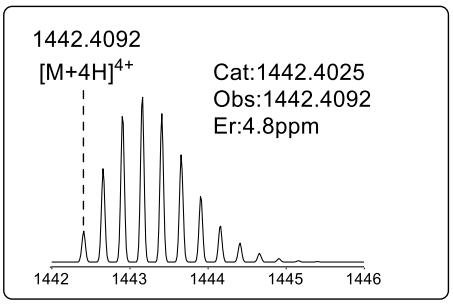
1442.4092
[M+4H]4+
Cat:1442.4025
Obs:1442.4092
Er:4.8ppm
1442
1443
1444
1445
1446

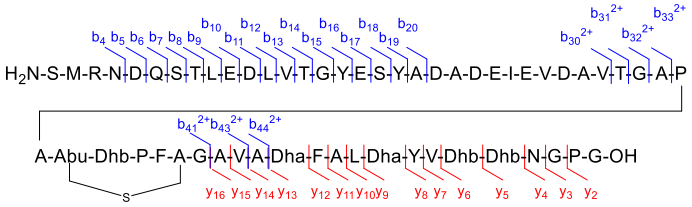
H2N-S-M-R-N-D-Q-S-T-L-E-D-L-V-T-G-Y-E-S-Y-A-D-A-D-E-I-E-V-D-A-V-T-G-A-P
A-Abu-Dhb-P-F-A-G-A-V-A-Dha-F-A-L-Dha-Y-V-Dhb-Dhb-N-G-P-G-OH
S

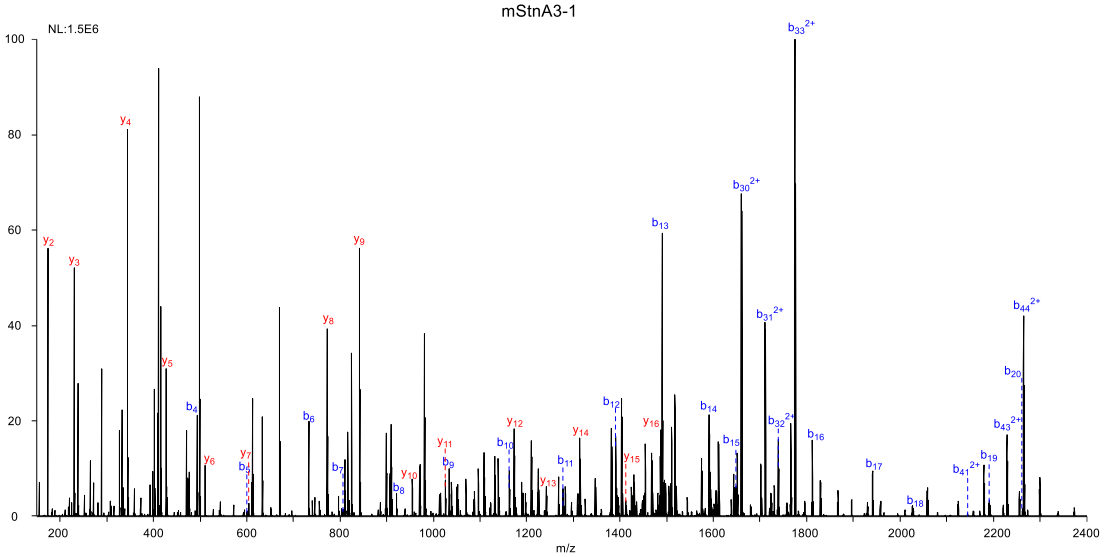
mStnA3-1
NL:1.5E6
m/z

Ions	Calc.	Obs.	Er.(ppm)	Ions	Calc.	Obs.	Er.(ppm)
b4	489.2244	489.2234	2.0	**y16**	1482.7183	1482.6831	23.7
b5	604.2513	604.2496	2.8	**y15**	1411.6812	1411.6987	12.4
b6	732.3099	732.3076	3.1	**y14**	1312.6128	1312.6314	14.2
b7	819.3419	819.3409	1.2	**y13**	1241.5757	1241.5943	15.0
b8	920.3896	920.3906	1.1	**y12**	1172.5588	1172.5718	11.1
b9	1033.4736	1033.4719	1.6	**y11**	1025.4905	1025.5035	12.7
b10	1162.5162	1162.5152	0.9	**y10**	954.4534	954.4667	13.9
b11	1277.5432	1277.5430	0.2	**y9**	841.3693	841.3823	15.5
b12	1390.6272	1390.6272	0.0	**y8**	772.3525	772.3618	12.0
b13	1489.6957	1489.6939	1.2	**y7**	609.2892	609.2976	13.8
b14	1590.7433	1590.7426	0.4	**y6**	510.2208	510.2300	18.0
b15	1647.7648	1647.7605	2.6	**y5**	427.1884	427.1929	10.5
b16	1810.8281	1810.8249	1.8	**y4**	344.1559	344.1558	0.3
b17	1939.8707	1939.8708	0.1	**y3**	230.1130	230.1130	0.0
b18	2026.9027	2026.9101	3.7	**y2**	173.0915	173.0918	1.7
b19	2189.9661	2189.9590	3.2				
b20	2261.0032	2261.0082	2.2				
b30^{2+}	1659.2358	1659.2372	0.8				
b31^{2+}	1709.7596	1709.7562	2.0				
b32^{2+}	1738.2704	1738.2705	0.1				
b33^{2+}	1773.7889	1773.7893	0.2				
b41^{2+}	2142.9421	2142.9582	7.5				
b43^{2+}	2227.9949	2228.0043	4.2				
b44^{2+}	2263.5134	2263.5256	5.4				

Figure. S20. MS analysis of mStnA3-1. The HR-MS, HCD fragments, and the MS/MS spectrum are shown.

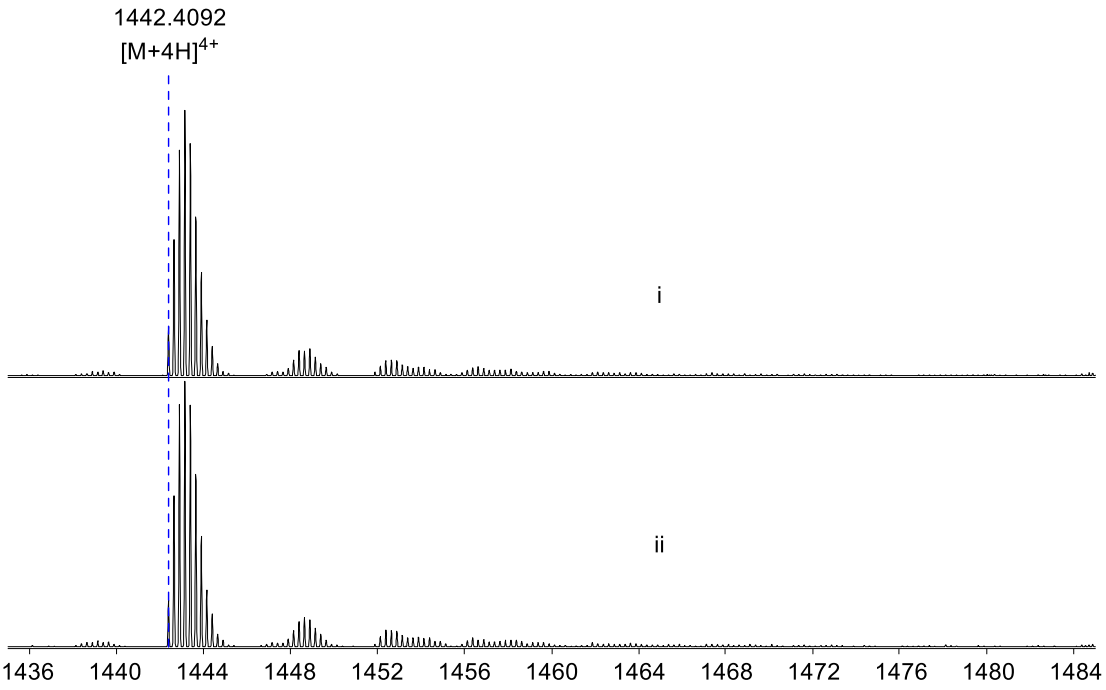

Figure. S21. Iodoacetamide derivatization of mStnA3-1. mStnA3-1(i), and mStnA3-1 + iodoacetamide (ii). The calculated $[M+4H]^{4+}$ for mStnA3-1 is 1442.4025.

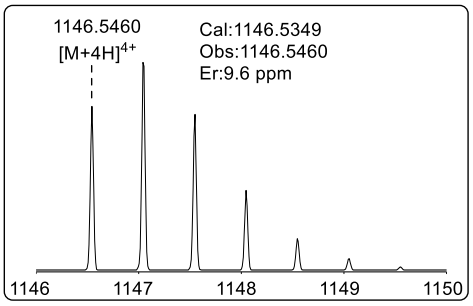
1146.5460
[M+4H]4+
Cal:1146.5349
Obs:1146.5460
Er:9.6 ppm
1146
1147
1148
1149
1150

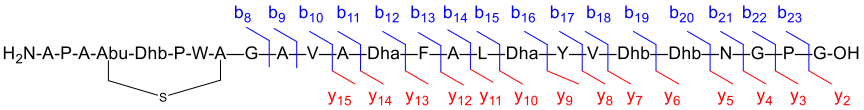
b8 b9 b10 b11 b12 b13 b14 b15 b16 b17 b18 b19 b20 b21 b22 b23
H2N-A-P-A-Abu-Dhb-P-W-A-G-A-V-A-Dha-F-A-L-Dha-Y-V-Dhb-Dhb-N-G-P-G-OH
S
y15 y14 y13 y12 y11 y10 y9 y8 y7 y6 y5 y4 y3 y2

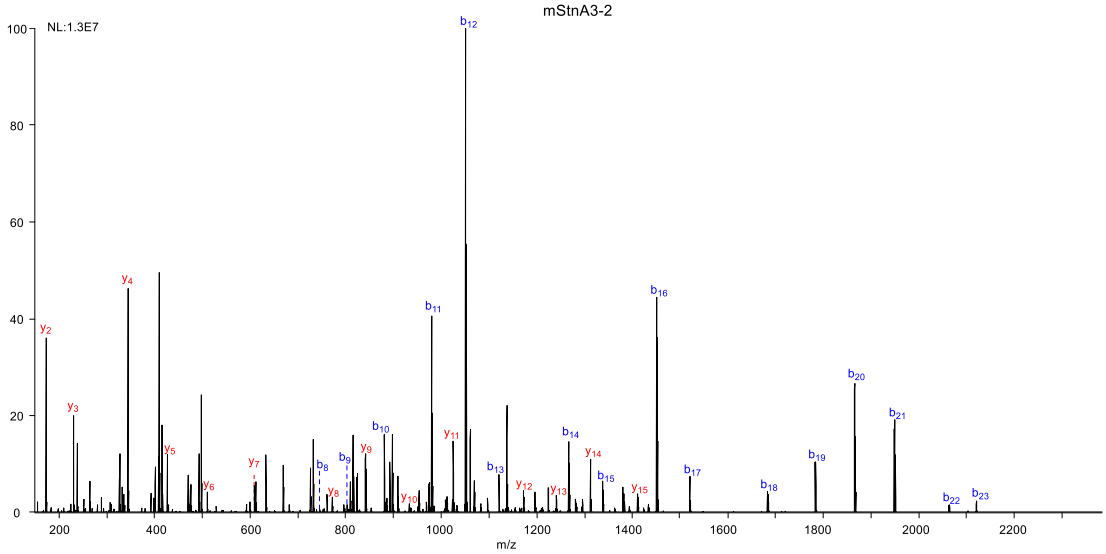
mStnA3-2
NL:1.3E7
100
80
60
40
20
0
200
400
600
800
1000
1200
1400
1600
1800
2000
2200
m/z
b12
y4
y2
b11
b16
y3
b20
b21
y5
b10
y11
b14
b19
y7
b9
y9
b8
y14
b15
b13
b17
y6
y12
y13
b18
y15
y10
b22
b23

Ions	Calc.	Obs.	Er.(ppm)	Ions	Calc.	Obs.	Er.(ppm)
b8	753.3300	753.3369	9.2	**y15**	1411.6812	1411.6955	10.1
b9	810.3515	810.3585	8.6	**y14**	1312.6128	1312.6279	11.5
b10	881.3886	881.3956	7.9	**y13**	1241.5757	1241.5925	13.5
b11	980.4570	980.4632	6.3	**y12**	1172.5588	1172.5705	10.0
b12	1051.4941	1051.5009	6.5	**y11**	1025.4905	1025.5027	11.9
b13	1120.5109	1120.5215	9.5	**y10**	954.4534	954.4651	12.3
b14	1267.5793	1267.5893	7.9	**y9**	841.3693	841.3820	15.1
b15	1338.6165	1338.6266	7.5	**y8**	772.3525	772.3607	10.6
b16	1451.7006	1451.7097	6.3	**y7**	609.2892	609.2983	14.9
b17	1520.7173	1520.7313	9.2	**y6**	510.2208	510.2299	17.8
b18	1683.7806	1683.7951	8.6	**y5**	427.1884	427.1926	9.8
b19	1782.8490	1782.8627	7.7	**y4**	344.1559	344.1556	0.9
b20	1865.8815	1865.8989	9.3	**y3**	230.1130	230.1129	0.4
b21	1948.9139	1948.9380	12.4	**y2**	173.0915	173.0917	1.2
b22	2062.9568	2062.9769	9.7				
b23	2119.9783	2119.9965	8.6				

Figure. S22. MS analysis of mStnA3-2. The HR-MS, HCD fragments, and the MS/MS spectrum are shown.

3. Supplementary Tables.

Table S1. Amino acid sequence of 158 precursor peptide candidates.

Accession	Sequence
	Subgroup 1
EDY62314.1	MDKTGAITELIEGYDSYSDAEELNSTAAAEAPATSAPCG AASVSWLASQFTVKTYKEGC
EDY62315.1	MADLQQTGSISELVAGYDTYSEAGELVAEAAADAPAST PTCAAATISWLGSQLTVKTYKEGC
WP_037654341.1	MEKVDSIMELLSGYETYSTVEEINLSAASDAPATTLVCA ATAGASWLTGQAVSKTYDEGC
WP_037848572.1	MEKATSIVELLSGYEAYSSVEEINLSAASDAPATTWGCA AVSASISWMSGQVVSKTVDDGC
WP_055704500.1	MEKATAIEDLMAGYEAYSDARELGVTSAVDAPATSPAC IASATASWLASQFSAKTISGGC
WP_067439886.1	MEKATSIVELLSGYEAYSSAEEINLSAATDAPATTWGCA AVSASVSWMSGQVVSKTVDDGC
WP_073921129.1	MEKATSVIELLSGYEAYASAEDINLSAASDAPATTWGC AAVSASISWMSGQVVSKTVDDGC
WP_130878494.1	MEKSEAIIDLMAGYDAYSSADELNTTAAAEAPASTPAC AAATMSWLGSQLTVKTYKDGC
WP_130878495.1	MEKSEAIMDLMAGYDAYSTVDELNTTAAADAPATTAP CGAATVSWLASQFTVKTYKDGC

WP_145487441.1	MEKTTAIMELMAGYEAYSDARELNVAAAAEAPATTPA CLASATASFVASQFSAKTIAGGC
WP_177150683.1	MEKASSIVELLSGYEAYSSPEDINLSAASDAPATTWGCA AVTASISWMSGQVVSKTIDDGC
WP_184734959.1	MEKSEAIMDLMAGYDAYSSVDELNTTAAADAPATSAP CGAAGVSWLASQFTVKTYKDGC
WP_189234319.1	MEKTTAIMELMAGYEAYSDARELNVTAAAEAPATSPAC IASATASFVASQFSARTIAGGC
WP_190198377.1	MEKTTAIMELMAGYEAYSDVRELNVTAAAEAPATSPAC IASATASFVASQFSARTIDGGC
WP_190198378.1	MEKTTAIMELMAGYEAYSDVRELNVTAAAEAPATSPAC IASATASYVASQFSAKTIAGGC
WP_229864334.1	MTTAITELMAGYEACSDVRELNVTAAAEAPATSPACIA GATASFVASRFSARTIDGGC
WP_239766125.1	MEKTTAIMELMAGYEAYSDARELNVTAAAEAPATSPAC LASATASFVASQFSAKTIAGGC
WP_266398935.1	MEKTTAIMELMAGYEAYSDARELNVTAAAEAPATSPAC LASATASFVASQFSARTIAGGC
WP_277332212.1	MEKTTAIMELMAGYEAYSDARELNVTAAAEAPATTPA CLASATASFVASQFSARTIAGGC
WP_277332214.1	MEKTTAIMELMAGYEAYSDARELNVTAAAEAPATTPA CLASATASFVASQFSAKTIAGGC

Subgroup 2	
WP_015659228.1	MNTAEQLIAGYAAYTNAEEFGASAGPDAPAITITTVSSP ECVYFSLSAVSGSIATTKSWGC
WP_015659229.1	MNTAEQLIAGYTAYTNAEEFGAGATAENPAITPTLLSFI GGSSGGCGGAVSAISGASVAGTVNWGC
WP_031041759.1	MNTSDNLMAGYATYTSADEIAATLDGGAPEISPVSLSIA VSITESSYACGAGISLSVGWTVGKGC
WP_053560634.1	MNASAHLIAGYTAYTTAAEFDASITADAPAVTPATPSIAL SIAESSYACGAGVGASIGITFTKGC
WP_071383935.1	MNTADQLIAGYTAYTSAEEFGVTAEGDAPATTPVTVTT VSSPECVQVSITVVGTTISGNC
WP_071383936.1	MNTADQLIAGYTAYTSAEEFGVTAEGDAPATTPSILVSI DMSSAACGATIGYSISKTVNGGC
WP_109497451.1	MNTTDTLLAGYAAYTSADEIAAAQDGGAPEISPVSLSIA VSIAESSYACSAGLSMSVGVTVGKGC
WP_128433858.1	MNTTENLIAGYTAYTSAQEIEATHAEEAPGATPSVLSFI ATSGWACGAGIGTSIGVTAAKGC
QDN59091.1	MNTADQLIAGYTAYTDAADFGASAAGEAPATTPSIITAS SPECGAFSISAASGILTSVSITHGAGC
QDN59092.1	MNTADQLIAGYTAYTDAADFGASAGGQAPATTPTILSVI AESTPACGGAVSAVSASAVGFTAHWGC
WP_153461214.1	MNNADQLIAGYTAYTDAEEVGAGATAEAPATTPALSVI

	AVSTAACGAAVGSAIGGSIAGTVNWGC
WP_215178513.1	MNTADQLLAGYTAYTTAEDFGASADNQSPAATPTITTV
	SSPECIYFSLGASAGSIASTKAWGC
WP_215178515.1	MNTADQLLAGYTAYTNAEEFGAGVSADAPAITPTVLSF
	IGGSSGGCGAAVSAISGAGVSATANWGC
WP_230901794.1	MNTTDQLISGYAAYATAEEVGAAQTTGAPEASPVALSA
	TVVITEGSYALSAGISMSAGVTFGKGC
WP_240117642.1	MNAADQLLEGYTAYTTAEEFGVAAESDAPAITTTVTSS
	EICVSLVSASVTATWDHGC
WP_266864817.1	MNTTDQLISGYAAYATAEEIGAGQMTGAPEASPVALSA
	TVVITEGSYALSAGISMSAGVTFGKGC
WP_306186810.1	MNTADQLIAGYTAYTDAADFGATAAGEAPATTPSIITAS
	SPECGAFTISAASGVLTSVSITHGAGC
WP_306186812.1	MNTADQLIAGYTAYTDAADFGATAGGQAPATTPSILSV
	VAESSAACGGAVSAVSAASVGFTAHWGC
	Subgroup 3
EFL08884.1	MHTMTETDLLSGYTAYTTAEELDQFDGKAAPAATTPVL
	APILIRASIIAARSSQQCAAGIAAAGGGIWRTIRKVC
WP_018960897.1	MQNVTEQDLFDGYTAYTSAEELGLHDGKDAAPAFSPTI
	PWAIRATIISARSSQQCAAALGSLAAKTVENKC
WP_031172570.1	MQSTQTEKDLFEGYTAYTSAEELGLYDGKDAAPAFSPT
	IPWAIRATIITARSSQQCAAALGSLTAKTIEKKC

WP_055513948.1	MQSTQNEKDLFEGYTAYTSAEELGLYDGKDAAPAFSPT IPWAIRATIITARSSQQCAAALGSLTARTIEKKC
WP_093908739.1	MQSTQNEKDLFEGYTAYTSAEELGLYDGKDAAPAFSPT IPWAIRATIITARSSQQCAAAIGSLTAKTIENKC
WP_100660920.1	MQNVTEKDLFDGYTAYTSAEELGLHDGATAGPAFSPTV PWAIQATVISARSSQACAAALGSLAAKTVEKKC
PSJ25815.1	MQNVTEKDLFDGYTAYTSAEELGLYDGKDAAPAFSPTI PWAIRATLITARSSQQCAMAIGSFTARTIESKC
PVD03988.1	MQTTQNEKDLFEGYTAYTSAEELGLYDGKDAAPAFSPT IPWAIRATIITARSSQQCAAALGSLTAKTIEKKC
WP_120754724.1	MQNVTEKDLFDGYTAYTSAEELGLYDGKDAAPAFSPTI PWAIRATLITARSSQQCAAAIGSFTARTIESKC
WP_124268919.1	MQNVTEKDLFDGYTAYTSAEELGLHDGKEAAPAFSPTI PWAIRATIITARSSQQCAAALGSLAAKTVENKC
WP_141310909.1	MQSTQNEKDLFEGYTAYTSAEELGLYDGKDAAPAFSPT IPWAIRATIITARSSQQCAAALGSLTAKTIEKKC
WP_179084717.1	MQNVTEKDLFDGYTAYTSAEELGLYDGKDAAPAFSPTI PWAIRAGLITARSSQQCAAAIGSFTARTIESKC
WP_217210041.1	MQSTQNEMDLFEGYTAYTSAEELGLYDGKDAAPAFSP TIPWAIRATIITARSSQQCAAAIGSLTAKTIENKC
WP_267088483.1	MQNVTEQDLFDGYTAYTSAEELGLHDGATAGPAFSPTV PWAIQATVISARSSQACAAALGSLAAKTVEKKC

WP_272114553.1	MQSTQNEKDLFEGYTAYTSAEELGLYDGKDAAPAFSPT IPWAIRATIITARSSQQCAAALGSLTAKTIENKC
	Subgroup 4
WP_030697775.1	MNTQSLISGYSAYATADEIVPAVEAPGATITITTSSQACIS AASAVSAVSIDNTFDHSC
WP_042175381.1	MNTESLIAGYSAYAAADEIVPAVEAPGATITITTSSQACI SAASAVSAVSIDNTFDHSC
WP_055421438.1	MNTQSLISGYSAYAAADEIVPAVEAPGATITITTSSQACI SAASAISAVSIDNTFDHSC
WP_078077248.1	MNTQSLISGYTSYADADELVPAVEAPGATITVTVTSSAA CISAASAISAVSIDNTFDHSC
WP_078077249.1	MNTQSLISGYTSYAEADELVPAAEAPGLIITTVTTSSQA CISAISAVSAVSIDNTFDHSC
WP_078077250.1	MNTQSLISGYASYADADELVPAVDAPGGTITITVTSSQA CISAASAISAVSIDNTFDHSC
WP_078878571.1	MGVNMNTESLIAGYSAYAAADEIVPAVEAPGATITITTS SQACISAASAVSAVSIDNTFDHSC
WP_159030605.1	MNTQSLISGYSTYAAADEIVPAVEAPAATITITTSSQACIS AASAVSAVSVDNTFDHSC
WP_179878856.1	MNAQSLISGYSTYAAADEIVPAVEAPAATITITTSSQACI SAASAVSAVSVDNTFDHSC
WP_189107027.1	MNTQSLISGYTSYADADELVPAVDAPGGTITVTVTSSQA

	CISAASAISAVSIDNTFDHSC
WP_210959286.1	MNTQSLISGYSTYAAADEIVPAVEAPGATITITTSSQACIS
	AASAVSAVSIDNTFDHSC
WP_216854818.1	MNTQSLISGYSAYADADELVPAVEAPGATITITTSSQACI
	SAASAISAVSIDNTFDHSC
WP_274816480.1	MNTQSLISGYSAYAAADEIVPAVEAPAATVTVTTSSAAC
	ISAASAVSAASVDNTFDHSC
	Subgroup 5
WP_166662147.1	MNEKLIAGYAAYTDAAELSAAALGEAPATIEIVTATVAS
	FVASAKTYDISC
WP_166662148.1	MNEKLIAGYAAYTDAAELSAAALDEAPATIEIVTATVAS
	FVASAETYDIKC
WP_166662149.1	MNEKLIAGYAAYTDADEFGTTALGEALASVESVSWVL
	SAASAGASVAATFDVGC
WP_181138636.1	MNEKLIAGYTAYTNADEYGATTLGDAPGSAESASWVL
	SAASLGASVAATFDKGC
WP_205034283.1	MNEKLIAGYAAYTNADEYGTAAAGEAPASIESVSWAVS
	GAAVGASVSASVKYGC
WP_205034285.1	MNEKLIAGYAAYTTADEYGTAAVGEAPASAETVTVGIT
	IASIGLSASTVTSKC
WP_214947142.1	MNEKLIAGYAAYTDAEEFAADALDGAPATIEIVSLTVAS
	FVASAKTYDIAC

WP_214947143.1	MNEKLIAGYAAYTNADEFAANVLDSAPATIEIISLTVASF VASAETYDIKC
WP_214947144.1	MNEKLIAGYAAYTDADEFGSTTLGDAPATIETVSWVVS AASVGASVAATFDVGC
Subgroup 6	
WP_114054643.1	MQNIENVEIMELVGGFEAYAQAAELNFEASADAPAITPT LTTIAYTKVTVAGTAASIKWTC
WP_125543401.1	MQKIENVNIMELVGGFEAYADAAELNFEASADAPAITP TLTTIAYTKVSVAAGTASWKYSC
WP_158070972.1	MQNDIEIMELVGGFEAYTEAAELNMEASVEAPAATPTA TIVYTKFSVASVTLTAKKGC
WP_159688188.1	MQKNDTVDIMELVGGFEAYAEAAELNFEASADAPAITP TLTTIAYTKVSVASVSASVKWGC
WP_249766625.1	MQKIENVDIMELVGGFEAYADAAELNFEASADAPAITP TLTTIAYTKVSVAATAASYKWSC
WP_266935718.1	MQKIENVNIMELVGGFEAYADAAELNFEASADAPAITP TITTIAYTKVSVAAGTASWKYSC
WP_272586646.1	MQNDIEIMELVGGFEAYTEAAELNMEASVQAPAATPTA TIVYTKFSVASVTLTAKKGC
Subgroup 7	
WP_158778660.1	MNDIELAAGFDTYADVNEMADEVTPDEAPSPQTIVSLS IVASVKWGC

WP_159392957.1	MNDIELAAGFDAYADVNEMADEVTPDEAPSPQTIISVIV TASFDC
WP_164496181.1	MNEIDLAAGFDTYADVNEMATEVTPDEAPSPQTIVSLS VVASIKWGC
WP_165890941.1	MNEIDLAAGFDTYADVNEMVADGTPDEAPSPQTIVSLS VVASIKWGC
WP_214947306.1	MNDVELATGFDAYADVNEMAAEVTPDEAPSPQTIISLSI VASFKWGC
WP_264245111.1	MNDIELAAGFDTYADVNEMADEVTPDEAPSPQTIVSLS VVASIKWGC
WP_289933485.1	MNDIELAAGFDTYADVNEMADEVTPDEAPSPQTIISLS VVSSIKWGC
Subgroup 8	
WP_158717266.1	MSHDQNTLEELVTGYESYADADEIEVDAVTGAPATTPF CGAAASFMLSYVTTNGPG
WP_158717267.1	MSNDQSMLEELVTGYESYADADEIEVDAVTGAPATTPF CGAVASFALSYVTTNGPG
WP_158717830.1	MRNDRSTLEDLVTGYESYADADEIEVDAVTGAPATTPF CGAVASFALSYVTTNGPG
WP_158754607.1	MTNDQSTLEDLVTGYESYADADEIEVDAVTGAPATTPF CGAVASFALSYVTTNGPG
WP_158879745.1	MRNDQSTLEDLVTGYESYADADEIEVDAVTGAPATTPF

	CGAVASFALSYVTTNGPG
WP_158879748.1	MRNDQSTLEDLVTGYESYADADEIEVDAVTGAPATTPF
	CGAAASFMLSYVTTNGPG
Subgroup 9	
WP_159425375.1	MNSNDSIMELVAGYETYMDADELDVTAVADAPATTWY
	CASAAASFISAATYEATC
WP_167346010.1	MNNTDSIMELVAGYETYMDASELDVNAVTDAPATTWY
	CVSAGVSFVTAATYEATC
WP_167751178.1	MNSNDSIMELVAGYETYMDANELDVTAVADAPATTWY
	CASAAVSFLSAATYEATC
WP_177150682.1	MNSTDSIMDLVAGYETYMDASELDVTAVADAPATTWY
	CASAAVSFLSAITYEATC
WP_199885689.1	MNNTDSVMDLVAGYQTYMDAGDLDVSAVADAPATTW
	YCASAAASFLSAVTYEATC
Others	
EDY62313.1	MSGPADAGPRIQENTMQNNTEIMDLIANYDAYADVDE
	LNVTAAADAPATTPVCAASVASSTWCASAASAISGATY
	EAGC
EFL15961.1	MDSMDLIAGYAAYTTPEELAASEATDAPAITTTVTSSEI
	CITITVGWGC
WP_030025843.1	MDNASMMDLVAGYNTYAEASELGIQAVADAPATTPVC
	AATVAASAVSSGWCASAAASAAGGATYKLGC

WP_030718520.1	MDNASMMDLVAGYNTYAEASELGIQAVADAPATTPVC
	AATIAASAVSSGWCASAAASAAGGATYKLGC
WP_037774183.1	MQNNTEIMDLIANYDAYADVDELNVTAAADAPATTPV
	CAASVASSTWCASAASAISGATYEAGC
WP_055704501.1	MDKSTAIMELVSNYTSYADVTELNVTAAADAPATTPVC
	AVSIASSSWCAAGASAASGATYEITC
SCE13261.1	MSAQDLMNGYALYTDAEELAAQVVDAPAQESSPICLSF
	ISGISVSLTAEHTC
WP_128433855.1	MNTADQLMAGYAVYTTSDEIGAGAAADAPAISPVSIFS
	AASSVECAIFSAGVVTSASAGGTVAGNC
WP_145487440.1	MDKSMAIMELVSNYDAYADVDELNISAAADAPATTPV
	CAVSVASSSWCAASASAASGATYELTC
WP_164497196.1	MDTHELIEGFDAYVEAEELNEDAMVDAPATTVPCTVAS
	FATGYFSC
WP_164992316.1	MSEQELIEGYRYFVDVAELAASAERELPTTSIFSYVTTT
	CTGTVATVSV
WP_164992317.1	MSAQDLMNGFAAYTDVEELAAQATTVTKEEASLSIGLS
	LSFISGVSVSLTAEHTC
WP_164992318.1	MTAHDLVEGYRTFADAEELAASPAGEYLPTTTIFTISYP
	TTATPTISN
WP_164992319.1	MSAQNLMNGFDAYTDAEELAAQPTTVTKEEQSMSLAI
	TLVTISVVHTYDTGC

WP_165451546.1	MDKTDAIMDLVSNYDAYADVAELNVTAAADAPATTPV CAATLASSGWCAAGASAISGATYEAGC
WP_169729690.1	MGEVVEMVAGFDTYADVEELNQIAVGEAPESSAPCTIY ASVSASISATASWGC
WP_184734957.1	MDKNNSIMDLVSNYDAYADVAELNVTAAADAPATTPV CAATLASSAWCAAGASAISGATYEAGC
WP_184823924.1	MDAVELFEGYSAYASTEEVAAADASEAPAITSTVTSSQG CAITVSAIFGC
WP_190198375.1	MDKSVAIMELVSNYDAYADVEELNISAATDAPATTPVC AATASSAPCAAAASAVSAVTYHKGC
WP_190198376.1	MDKSVAIMELVSNYDAYADVDELNISAAADAPATTPVC AASVASSSWCAASASAVSGATYELTC
WP_209340438.1	MTDQLIEGYAAYASAEEIQAAGQAPATPVTVALSIAGSA LSGAGVGVSIGESIKHSC
WP_209340439.1	MTQDLISGYAAYAEADELVAATGEAPATPVTIAISGAFST SLAASAATVAGNC
WP_227957703.1	MDTQSLISGYAAYAEAEEIAPAAEAPAATTTVTTSSQACI SAISAVSAVSVDNTFDHSC
WP_239766123.1	MDKSMAIMELVSHYDAYADVDELNITAAADAPATTPV CAASVASSSWCAASASAVSGATYELTC
WP_243146557.1	MAGYTAYTSAAELGAAVDEAPAYTPTLSITGTCMTPILT LVNGC

WP_266398929.1	MDKSLAIMELVSHYDAYADVDELNMTAAADAPTSTPV CAVSVASSSWCAASASAVSGATYELTC
WP_266398932.1	MDKSLAIMELVSHYDAYADVDELNMTAAADAPASTPV CAVSVASSSWCAASASAVSGATYELTC
WP_266679587.1	MAAAELIEGYAMYVSPEEADSLQIPDLDVEGQSIPPTPI ATTLIVHC
WP_277332213.1	MDKSMAIMELVSNYDAYADVDELNITAAADAPATTPV CAASIASSSWCAASASAVSGATYELTC

Table S2. Proposed function for each protein encoded in the *stn* gene cluster.

Protein	Length (AA)	Closest BLAST homolog (GenBank accession number)	Putative function
StnR	320	WP_052680418.1	Regulator
StnU1	110	WP_030028050.1	Hypothetical protein
StnP	844	WP_075970604.1	Putative Zn-dependent peptidase
StnX	320	WP_075970605.1	Hypothetical protein
StnD	199	WP_045320845.1	Flavoprotein
StnJ	320	WP_030025853.1	LLM class F_{420}-dependent oxidoreductase
StnT3	611	WP_075970606.1	ABC transporter
StnT2	407	WP_030025848.1	ABC transporter
StnT1	295	WP_075970607.1	ABC transporter
StnM	349	WP_030025845.1	*N*-Methyltransferase
StnA3	56	WP_158879745.1	Precursor peptide
StnA2	56	WP_158717266.1	Precursor peptide
StnA1	68	WP_030025843.1	Precursor peptide
StnY	350	WP_079273209.1	Class V dehydratase subunit LanY
StnK	368	WP_030025841.1	Class V dehydratase subunit LanK
StnU2	119	WP_075970608.1	Hypothetical protein

Table S3. ^{1}H (500 MHz) and ^{13}C NMR (125 MHz) Data for **1**.

No.	Position	δ_H mult. (*J* in Hz)	δ_C	No.	Position	δ_H mult. (*J* in Hz)	δ_C
NMe_2Abu(*S*)-1	CON	—	172.1		3	—	110.1
	Me2	2.94 s	40.1		4	7.54 d (7.5)	118.2
		2.83 s	43.6		5	6.97 t (7.5)	118.4
	α	4.19 br d (4.2)	71.9		6	7.05 t (7.5)	121.0
	β	3.65[a]	39.8		7	7.33[a]	111.4
	γ	1.32 d (7.0)	17.3		8	—	136.0
Dhb-2	CON	8.35 s	164.7		9	—	127.2
	α	—	127.1	Ala(*S*)-19	CON	7.70[a]	171.9
	β	5.90 q (7.0)	126.1		α	4.33[a]	53.6
	γ	1.46 d (7.0)	14.2		β	2.93[a]	33.8
Pro-3	CO	—	171.2			2.86[a]	
	α	4.45[a]	64.0	Ala-20	CON	8.06[a]	172.1
	β	2.28, m	32.1		α	4.18[a]	57.4
		1.88[a]			β	1.19[a]	17.8
	γ	1.87[a]	23.0	Ala-21	CON	8.15[a]	172.0
		1.81[a]			α	4.37[a]	48.4
	δ	3.89[a]	47.1		β	1.27[a]	18.5
		3.37[a]		Ala-22	CON	8.12[a]	171.9
Val-4	CON	7.90[a]	173.7		α	4.36[a]	48.4
	α	4.55 t (8.6)	56.6		β	1.26[a]	17.6
	β	2.00 m	31.6	Ala-23	CON	8.01[a]	172.0
	γ	0.80[a]	18.5		α	4.23[a]	48.4
	δ	0.85[a]	19.3		β	1.24[a]	17.9
Ala(*S*)-5	CON	8.98 d (9.6)	168.6	Ala-24	CON	8.00[a]	171.9
	α	4.92 t (11.1)	52.1		α	4.22[a]	48.3
	β	3.36[a]	38.3		β	1.23[a]	17.8
		2.62[a]		Ala-25	CON	8.38[a]	171.7
Ala-6	CON	8.08[a]	171.4		α	4.20[a]	48.3
	α	4.36[a]	48.4		β	1.17[a]	17.6
	β	1.25[a]	18.4	Ala-26	CON	8.17[a]	172.0
Ala-7	CON	8.11[a]	171.9		α	4.20[a]	48.2
	α	4.21[a]	48.3		β	1.19[a]	17.8
	β	1.20[a]	19.5	Ala-27	CON	8.15[a]	171.4
Abu-8	CON	7.87[a]	171.5		α	4.37[a]	48.8
	α	4.33[a]	53.5		β	1.24[a]	18.0
	β	1.67 m	26.0	Gly-28	CON	8.07[a]	172.6

	γ	0.80[a]	9.9		α	3.76[a]	42.1
Val-9	CON	8.06[a]	170.9			3.73[a]	
	α	4.18[a]	57.4	Gly-29	CON	8.11[a]	172.5
	β	1.96[a]	30.6		α	3.81[a]	42.2
	γ	0.80[a]	18.5			3.71[a]	
		0.85[a]	19.3	Ala-30	CON	8.15[a]	172.0
Ala -10	CON	8.05[a]	172.1		α	4.37[a]	48.5
	α	4.19[a]	48.5		β	1.27[a]	17.6
	β	1.20[a]	18.0	*allo*AviMe Cys-31	CON	8.32 d (8.9)	169.8
Ala -11	CON	8.02[a]	172.1		*α*	4.21[a]	56.2
	α	4.18[a]	48.6		*β*	3.22[a]	44.6
	β	1.18[a]	17.7		γ	1.19[a]	19.5
Ala -12	CON	8.05[a]	172.1		1’	5.33 d (8.5)	105.4
	α	4.19[a]	48.5		2’	6.67 t (8.5)	121.6
	β	1.20[a]	18.0		N-3’	8.75 s	—
Ala -13	CON	7.90[a]	172.0	Tyr-32	CON	8.70[a]	169.9
	α	4.16[a]	48.6		*α*	3.63[a]	57.9
	β	1.22[a]	17.6		*β*	3.12[a]	32.8
Val-14	CON	7.87[a]	169.6		1’	—	129.1
	α	4.15[a]	58.0		2’, 6’	6.86 d (8.2)	130.0
	β	2.08[a]	30.1		3’, 5’	6.59 d (8.2)	115.2
	γ	0.85[a]	14.0		4’	—	155.7
	δ	0.86[a]	14.2	Lys-33	CON	8.10[a]	169.4
Ala(*S*)-15	CON	7.77[a]	170.0		α	4.44[a]	51.3
	α	4.45[a]	53.9		β	2.28[a]	32.1
	β	2.99[a]	41.4			1.88[a]	
		2.90[a]			γ	1.87[a]	23.0
Dha-16	CON	9.58[a]	166.3		δ	1.87[a]	23.0
	α	—	136.4			1.81[a]	
	β	5.39 s	108.3		*ε*	3.89[a]	47.1
		5.43 s				3.37[a]	
Gly-17	CON	8.90[a]	169.6	Leu-34	CON	8.66[a]	172.9
	α	3.81[a]	44.0		*α*	3.98 m	53.0
		3.59[a]			*β*	1.45[a]	38.8
Trp-18	CON	8.04[a]	171.7		*γ*	1.54 m	24.1
	α	4.49[a]	54.6		*δ*	0.84[a]	19.3
	β	3.30[a]	26.4			0.90 d (6.6)	22.4
		3.11[a]		Gly-35	CON	8.76[a]	169.0
	NH-1	10.86 s	—		α	3.85[a]	43.3
	2	7.15 br s	123.5			3.59[a]	

[a] Overlapped signals

Table S4. ^{1}H (500 MHz) and ^{13}C NMR (125 MHz) Data for **3**.

No.	Position	δ_H mult. (*J* in Hz)	δ_C	No.	Position	δ_H mult. (*J* in Hz)	δ_C
NMe_2Abu(*S*)-1	CON	—	172.0		3', 5'	7.22[a]	127.9
	Me2	2.96 s	40.4		4'	7.16[a]	126.3
		2.82 s	43.7	Ala-12	CON	8.07[a]	171.5
	α	4.29 br d (4.2)	71.8		α	4.24[a]	58.3
	β	3.62 dq (7.2, 4.2)	40.2		β	0.90[a]	18.4
	γ	1.31 d (7.2)	17.9	Leu-13	CON	7.87[a]	170.9
Dhb-2	CON	8.71 s	162.4		α	4.27[a]	48.0
	α	—	127.1		β	1.99[a]	29.4
	β	5.81 q (6.8)	125.7			1.85[a]	
	γ	1.41 d (6.8)	14.1		γ	1.96[a]	30.5
Pro-3	CO	—	171.8		δ	0.76 d (6.8)	18.0
	α	4.20[a]	63.7		ε	0.79 d (7.1)	19.3
	β	1.86[a]	31.3	Ala-14	CON	8.27[a]	170.9
		1.24[a]			α	4.27[a]	48.2
	γ	1.76[a]	22.8		β	1.19[a]	18.4
		1.64[a]		Tyr-15	CON	8.20[a]	170.9
	δ	3.85[a]	46.9		*α*	4.55[a]	53.6
		3.29[a]			*β*	2.89[a]	36.4
Phe-4	CON	8.07 d (9.5)	174.5			2.59[a]	
	α	5.08 td (11.7, 3.5)	52.4		1'	—	137.3
	β	2.98[a]	38.5		2', 6'	7.01[a]	130.3
		2.86[a]			3', 5'	6.61[a]	114.7
	1'	—	137.3		4'	—	155.7
	2', 6'	7.29 d (7.2)	129.5	Val-16	CON	8.06[a]	170.9
	3', 5'	7.28[a]	127.8		α	4.24[a]	58.3
	4'	7.17[a]	127.8		β	2.06 m	30.3
Ala(*S*)-5	CON	9.28 d (9.3)	169.1		δ	0.90[a]	13.7
	α	4.97 br t (11.3)	52.4		ε	0.91[a]	13.7
	β	3.37[a]	39.8	Dhb-17	CON	9.47 s	164.3
		2.60[a]			α	—	131.0
Gly-6	CONH	8.29[a]	168.0		β	6.22 q (6.7)	125.7
	α	3.89[a]	41.8		γ	1.69 d (6.7)	12.9
		3.81[a]		Dhb-18	CON	9.06 s	163.8
Ala-7	CON	8.23 d (7.1)	172.1		α	—	130.4
	α	4.39[a]	48.1		β	6.45 q (7.0)	129.3
	β	1.19 d (7.3)	18.4		γ	1.66 d (7.	13.1

						0)	
Val-8	CON	7.88[a]	170.5	Asn-19	CON	7.88[a]	171.0
	α	4.12 t (7.5)	57.4		α	4.64 m	50.0
	β	1.94 m	30.5		β	2.61[a]	37.0
	γ	0.78 d (6.6)	17.9			2.52[a]	
	δ	0.81 d (6.6)	19.3		γ	—	171.8
Ala-9	CON	7.98 d (6.8)	171.4		NH_2	7.29[a], 6.93 (s)	—
	α	4.20[a]	48.3	Gly-20	CON	7.71[a]	169.1
	β	1.14 d (6.9)	18.3		α	3.88[a]	41.6
Ala -10	CON	7.76 d (7.5)	171.7			3.70[a]	
	α	4.24[a]	58.3	Pro-21	CON	—	172.0
	β	0.87 d (7.1)	18.7		α	4.29[a]	59.6
Phe-11	CON	8.19[a]	171.8		β	1.85[a]	29.3
	α	4.55[a]	53.6			1.99[a]	
	β	3.01[a]	37.8		γ	1.86[a]	24.0
		2.69[a]		Gly-22	CON	8.14[a]	172.0
	1’	—	137.8		α	3.72[a]	40.6
	2’, 6’	7.22[a]	129.3			3.71[a]	

[a] Overlapped signals

Table S5. Related bacterial strains and plasmids used in this study.

Strain/plasmid	**Characteristics**	**Source/References**
Streptomyces		
S. coelicolor M1152	Heterologous expression host	Routine preservation
STN-01 (WT)	Heterologous expression of *stnU1/K/Y/M/A1/A2/A3/J/D/X/P/U2* in *S. coelicolor*	This study
STN-02 (Δ*stnA2A3*)	STN-01 derivative in which *stnA2* and *stnA3* was deducted	This study
STN-03 (Δ*stnA1A3*)	STN-01 derivative in which *stnA1* and *stnA3* was deducted	This study
STN-04 (Δ*stnA1A2*)	STN-01 derivative in which *stnA1* and *stnA2* was deducted	This study
STN-05 (Δ*stnK*)	STN-01 derivative in which *stnK* was deducted	This study
STN-06 (Δ*stnY*)	STN-01 derivative in which *stnY* was deducted	This study
STN-07 (Δ*stnM*)	STN-01 derivative in which *stnM* was deducted	This study
STN-08 (Δ*stnD*)	STN-01 derivative in which *stnD* was deducted	This study
STN-09 (Δ*stnX*)	STN-01 derivative in which *stnX* was deducted	This study
STN-10 (*stnA2:stnA3*)	STN-01 derivative in which *stnA2* was engineered to code for *stnA3* core sequence	This study

STN-11 (Δ*stnA1A2M*)	STN-04 derivative in which *stnM* was deducted	This study
STN-12 (*stnA1*(T8S))	STN-01 derivative in which *stnA1* was engineered to code for StnA1-T8S	This study
E. coli		
DH5α	Host for general cloning	Transgen
ET12567/pUZ8002	Donor strain for conjugation between *E. coli* and *Streptomyces*	Ref. 9
BL21(DE3)	Host for protein expression	Transgen
Plasmids		
pRSFDuet-1	Protein coexpression vector used in *E. coli*, encoding N-terminal 6 × His tag, kanamycin resistance	Novagen
pETDuet-1	Protein coexpression vector used in *E. coli*, encoding N-terminal 6 × His tag, ampicillin resistance	Novagen
pXY200-1	Protein coexpression vector used in *Streptomyces*	Ref. 9
pXYDuet-*stn*	pXY200-1 derivative used for STN-01	This study
pXYDuet-Δ*stnA2A3*	pXYDuet-*stn* derivative used for STN-02	This study
pXYDuet-Δ*stnA1A3*	pXYDuet-*stn* derivative used for STN-03	This study

pXYDuet-Δ*stnA1A2*	pXYDuet-*stn* derivative used for STN-04	This study
pXYDuet-Δ*stnK*	pXYDuet-*stn* derivative used for STN-05	This study
pXYDuet-Δ*stnY*	pXYDuet-*stn* derivative used for STN-06	This study
pXYDuet-Δ*stnM*	pXYDuet-*stn* derivative used for STN-07	This study
pXYDuet-Δ*stnD*	pXYDuet-*stn* derivative used for STN-08	This study
pXYDuet-Δ*stnX*	pXYDuet-*stn* derivative used for STN-09	This study
pXYDuet-*stnA2:stnA3*	pXYDuet-*stn* derivative used for STN-10	This study
pXYDuet-Δ*stnA1A2M*	pXYDuet-Δ*stnA1A2* derivative used for STN-11	This study
pXYDuet-*stnA1*(T8S)	pXYDuet-*stn* derivative used for STN-12	This study
pRSFDuet-1-s*tnA3-stnKY*	pRSFDuet-1 derivative, containing *stnA3*, *stnK*, and *stnY*	This study
pRSFDuet-1-s*tnA1-stnKY*	pRSFDuet-1 derivative, containing *stnA1*, *stnK*, and *stnY*	This study
pETDuet-1-s*tnD*	pETDuet-1 derivative, containing *stnD*	This study
pETDuet-1-s*tnX*	pETDuet-1 derivative, containing *stnX*	This study

pETDuet-1-s*tnD-stnX*	pETDuet-1 derivative, containing *stnD* and *stnX*	This study

Table S6. Primers and chemically synthesized DNA sequences used in this study.

Primer	Sequence
pRSF-2-StnK-F	GAACAGATTGGTATGTCGACCACATTCGCTCC
pRSF-2-StnK-R	AGAACCACCACCAGAACCACCACCCGGGGTTACCTC CAATCCG
pRSF-2-StnY-F	GGTGGTGGTTCTGGTGGTGGTTCTGTGAGCACGGGAA CGAGAAC
pRSF-2-StnY-R	GCAGCGGTTTCTTTACCAGACTCGAGTACTGAGGTGG AAGCAGGGAG
pRSF-1-sumo-F	CTCGGCGCGCCTGCAGGTCGACAAGCTTATGTCGGAC TCAGAAGTCAATCAAGAAGC
pRSF-1-sumo-R	CGTTTCTCATGGATCCACCAATCTGTTCTC
pRSF-2-sumo-F	GTATAAGAAGGAGATATACATATGTCGGACTCAGAAGT CAATCAAGAAG
pRSF-2-sumo-R	TGGTCGACATACCAATCTGTTCTCTGTGAGCC
pRSF-StnA1-F	TTGGTGGATCCATGAGAAACGACCAGAGCACG
pRSF-StnA1-R	CGTTTCTCATGGATCCACCAATCTGTTCTC
pRSF-StnA3-F	TTGGTGGATCCATGAGAAACGACCAGAGCACG
pRSF-StnA3-R	CGTTTCTCATGGATCCACCAATCTGTTCTC
pETDuet-1-sumo-F	AACTTTAAGAAGGAGATATACATGTCGGACTCAGAAG TCAATCAAG
pETDuet-1-sumo-StnD-R	CGGCCGCAAGCTTGTCGACCTCACAGCGTGCTCGCCG
pETDuet-2-sumo-F	GTATAAGAAGGAGATATACAATGTCGGACTCAGAAGT CAATCAAG
pETDuet-2-sumo-R	TGGCGGTCACGGATCCACCAATCTGTTCTCTGTGAG
pETDuet-2-StnX-F	TGGTGGATCCGTGACCGCCACCCCCAC

pETDuet-2-StnX-R	CAGCGGTTTCTTTACCAGACTCAGTGGTCTCCTGGTGC

4. References.

(1) Kieser, T.; Buttner, MJ.; Charter, KF; Hopwood, D; Bibb, M. J.; Büttner, M; Chater, K. F.; Bibb, MJ; Chater, KF; Hopwood, DA; Bibb, M.J.; Buttner, M.J.; Hopwood, D.A.; Chater, K.F.; Bib, M.J.; Keiser, T; Butner, MJ; Bipp, MJ; Chater, K.F.; Chatter, KF; Kieser Y. *Practical Streptomyces Genetics* (John Innes Foundation, **2000**)

(2) Shang, Z.; Winter, J. M.; Kauffman, C. A.; Yang, I.; Fenical, W. Salinipeptins: integrated genomic and chemical approaches reveal unusual D-amino acid-containing ribosomally synthesized and post-translationally modified peptides (RiPPs) from a great salt lake *Streptomyces* sp.. *ACS Chemical Biology*. **2019,** *14*, 415-425.

(3) Vijayasarathy, S.; Prasad, P.; Fremlin, L. J.; Ratnayake, R.; Salim, A. A.; Khalil, Z.; Capon, R. J., C3 and 2D C3 Marfey's Methods for Amino Acid Analysis in Natural Products. *Journal of Natural Products* **2016**, 79 (2), 421-427.

(4) Georgiou, M. A.; Dommaraju, S. R.; Guo, X.; Mast, D. H.; Mitchell, D. A., Bioinformatic and Reactivity-Based Discovery of Linaridins. *ACS Chemical Biology* **2020**, 15 (11), 2976-2985.

(5) Chu, L.; Cheng, J.; Zhou, C.; Mo, T.; Ji, X.; Zhu, T.; Chen, J.; Ma, S.; Gao, J.; Zhang, Q., Hijacking a Linaridin Biosynthetic Intermediate for Lanthipeptide Production. *ACS Chemical Biology* **2022**, 17 (11), 3198-3206.

(6) C. L. M. Gilchrist, T. J. Booth, B. van Wersch, L. van Grieken, M. H. Medema, Y.-H. Chooi, A. Ouangraoua, *Bioinformatics Advances* **2021**, 1, vbab016.

(7) Zallot, R.; Oberg, N.; Gerlt, J. A., The EFI Web Resource for Genomic Enzymology Tools: Leveraging Protein, Genome, and Metagenome Databases to Discover Novel Enzymes and Metabolic Pathways. *Biochemistry* **2019**, 58 (41), 4169-4182.

(8) Crooks, G. E.; Hon, G.; Chandonia, J.-M.; Brenner, S. E., WebLogo: A Sequence Logo Generator. *Genome Research* **2004**, 14 (6), 1188-1190.

(9) Xue, Y.; Wang, X.; Liu, W., Reconstitution of the Linaridin Pathway Provides Access to the Family-Determining Activity of Two Membrane-Associated Proteins in the Formation of Structurally Underestimated Cypemycin. *Journal of the*

American Chemical Society **2023**, 145 (12), 7040-7047.